PRELIMINARY GEOPHYSICAL INVESTIGATION OF THE SOURCE OF HEAT OF THE WIKKI WARM SPRING, BAUCHI, NIGERIA.

BY

OMANGA UNCLE STEVE ATIMI

A thesis submitted to the Department of Physics, Ahmadu Bello University, Zaria, in partial fulfilment for the award of the Degree of Master *of Science in Applied Geophysics*

Dept. Of Physics
Ahmadu Bello University
Zaria, Nigeria.

March,1998

DECLARATION

I hereby declare that this thesis is an original work carried out by the author under the supervision of Dr. B.B.M. Dewu, and Prof. C.O. Ajayi. All the work of others are cited and duly acknowledged and referenced.

This thesis has not been submitted in whatever form to any other institution, organisation or body other than Ahmadu Bello University, Zaria, Nigeria for the award of any degree.

Omanga, U.S.A.

28-07-98
Date

CERTIFICATION

This project report entitled PRELIMINARY GEOPHYSICAL INVESTIGATION OF THE SOURCE OF HEAT OF THE WIKKI WARM SPRING, BAUCHI, NIGERIA by Omanga U.S.A meets the regulations governing the award of degree of Master of Science (M.Sc.), in Applied Geophysics of Ahmadu Bello University and is approved for its contributions to knowledge and literary presentation.

Dr. B.B.Muhammad Dewu
Chairman,
Supervisory Committee
Date 3/11/98

Prof. C.O. Ajayi
Member,
Supervisory Committee
Date 3/11/98

Prof. I.B. Osazuwa
Head,
Department of Physics
Date 05/11/98

Prof. J.Y. Olayemi
Dean,
Posgraduate School
Date 25/2/99

DEDICATION

To my children.

ACKNOWLEDGEMENTS

Thanks be to God who teaches man what he does not know. The author wishes to extend his sincere gratitude to all who in one way or the other helped in the success of this work the list of which is too numerous to mention here. In this respect, I would like to be thankful to Dr. B.B.Muhammad Dewu, for his patience and who supervised this work under strong criticism and friendly advice. Special thanks go to him for the information provided me during this write up and all round encouragement which led to successful completion of the work.

I am grateful to Professor Ajayi, C.O. my co-supervisor for the assistance given me during this work and for his comments and suggestions that were of immense help in the preparation of this thesis.

My sincere gratitude to the Head of Physics, ABU, Zaria, Prof. I. B. Osazuwa who made the departmental equipments available for the field work. I wish to also acknowledge Prof. Osazuwa's advice, suggestions and support which in no small measure helped to make this work possible. I am indebted to him for gratiously taking his invaluable time in reading through the thesis and making major contributions which helped in the preparation of the thesis. I wish to also express my profound gratitude to Mallam Mijiyawa, for his assistance in this work. I am also indebted to all my colleagues in the Physics Department especially

Dogara, M.E. and my friends who in one way or the other contributed to the success of the work.

My gratitude also goes to my employer university and the key officers, the Dean of Science, Professor E.C. Agishi and my Head of Department Dr. J.O. Fiase all of Benue State University, Makurdi whose consistent advice and encouragement made this work what it is.

I also appreciated the efforts of my able field assistants in the persons of Mr.Basil Nwosu, Atsinafe Omanga and the able Driver Mr. Gabriel Adzembe. I want to especially thank Mr. John Eka and family for tracing all the Figures and hospitality given me while in Zaria. Also my thanks goes to Itsoga Agishi who typed the work.

My gratitude also goes to the management of the Yankari National Park, Bauchi, who allowed me and my field assistants free entry to the Reserve and 50% discount in accomodation throughout my stay in the field and the members of staff who were very accomodating and co-operative.

Finally, I wish to express my gratefulness to my wives Helen Ayineka and Helen Atana whose all round support I enjoyed throughout the stages of this work.

ABSTRACT

Resistivity and radiometric methods of survey employing vertical electrical soundings (VES), and gamma ray spectrometry were carried out in the Wikki Warm Spring area. These were used with the aim of investigating the source of heat which Teats the water in the Wikki Warm Spring.

Within the Wikki warm spring area, fourteen (14) soundings were carried out using the conventional VES method. Radiometric; measurements were carried out from which the concentrations of the three radio-elements K, U, and Th in the area were estimated. These surveys were carried out with the aim of identifying the origin of the source of heat which heats the water in the Wikki warm spring, the investigation was also concerned with the point where this heating takes place, that is, whether the water is heated in the immediate vicinity of the spring or at some distant point.

Results from the interpretation of the data obtained led to the production of a number of graphs and maps from which conclusions were drawn. The resistivity results show that rather low resistivity values exist around the Wikki Spring area. This was interpreted as indicating that the Wikki area is underlain by water. The low resistivity values were recorded further away from the point where water is gushing out from the spring. The radiometric survey measurements reveal high gamma activity in this region. This higher than average radioactivity in the area is indicative of the

importance of radiogenic heat in the Wikki area. The high concentration of the radioelements K, U, Th points to the fact that the source heat of the Wikki warm spring is most probably due to the radioactivity.

TABLE OF CONTENTS

	Page
Title Page	i
Declaration	ii
Dedication	iii
Certification	iv
Acknowledgements	v
Abstract	vii
Table of contents	ix
List of Tables	xi
List of Figures	xii
CHAPTER ONE: INTRODUCTION	**1**
1.1 Hot Springs	1
1.2 The Wikki Warm Spring	4
1.2.1 Location of the Area	5
1.2.2 Geology of the Yankari Area	12
1.3 Aims and Objectives of the Study	13
CHAPTER TWO: GEOTHERMAL ENERGY	**17**
2.1 The Nature and Occurence of Geothermal Energy	17
2.2 Source Heat in Warm Springs	20
2.3 Heat Transfer in the Earth	26
2.4 Geothermal Energy Resources	27
CHAPTER THREE: RESISTIVITY AND RADIOMETRICS IN GEOTHERMAL RESOURCE EVALUATION	**31**
3.1 Resistivity Surveys: Principle, Techniques and Application	31
3.1.1 Computation of Apparent Resistivity	39
3.1.2 Choice of Electrode Arrangements	40
3.2 Field Procedure in Resistivity	42
3.3 Field Procedure in Radiometrics	44
3.3.1 Radioelement Concentration	45
3.4 Problems Encountered in the Field and Limitation of this Work	47
CHAPTER FOUR: INTERPRETATIONS AND DEDUCTIONS	**49**
4.1 Data Processing	49
4.2 Interpretation of the Resistivity Survey Results	50

4.2.1 Resistivity Values..... 54
4.2.2 Geoelectric and Geologic Sections..... 54
4.2.3 Geoelectric and Geologic Sections for VES P2/3, P5/9, P6/8, P7/10, P8/5..... 58

4.3 Maps Produced from Interpreted Data..... 59

4.3.1 Resistivity Map of the Surface Layer.. 59
4.3.2 Isoresistivity Map at AB/2 = 25m and at AB/2 = 35m..... 61

4.4 Results of Radioactivity Measurements..... 63

CHAPTER FIVE: DISCUSSION, SUGGESTIONS AND CONCLUSIONS **71**

5.1 Discussion..... 71
5.2 Conclusion 72
5.3 Suggestions for Further Work in the Area ... 73

REFERENCES..... 75
APPENDICES..... 78

LIST OF TABLES

Table		Page
1	Heat productivities of radioactive elements (after Birch, 1954)	23
2	Typical heat production in rocks (Bullard, 1969)	23
3.	Geothermal resources classification (White *et al.*, 1975)	29
4.1	Resistivity values for sedimentary rocks (Telford, *et al.*, 1975).....	57
4.2	Resistivity values used in deriving the geologic sections in this work (Telford, *et al.* 1975).....	57
4.3	The concentration of gamma-ray activity in the Wikki area (Profile 1).....	70

LIST OF FIGURES

Figure		Page
1.1	Schematic cross-section through Wikki warm spring	6
1.2	Schematic cross-section through Tungan Maliki salt lick and gold spring	7
1.3	Location map of Wikki warm spring at Yankari Game Reserve	8
1.4	Location of the Yankari Game Reserve within vital area for the surface water protection	9
1.5	Yankari Game Reserve, map showing groundwater table at peak of the wet season and directions of groundwater flow	11
1.6	Geological map of Yankari game Reserve	14
3.1	Resistivity configuration	32
3.2	Schematical diagram of the Wenner (a) and Schlumberger (b) arrangements	43
4.1	Resistivity plot for VES P1.....	53
4.2a,b	Geoelectric and Geologic sections for VES points 5, 11, 10, 8, 9 and 3.....	55
4.3	Contour map of the surface layer resistivity.....	56
4.4a	Isoresistivity contour map of the study area at AB/2=25m	61
4.4b	Isoresistivity contour map of the study area at AB/2=35.....	62
4.5	Contour map of the total count.....	65
4.6	Contour map showing areas of %k concentrations.....	66
4.7	Contour map showing areas of eU concentrations.....	67
4.8	Contour map showing areas of eTh concentrations.....	68

Chapter One

INTRODUCTION

1.1 Hot springs

Ground water reaching great depths into the earth may be heated to temperatures far above the boiling point of water, which is 100°C at sea-level atmospheric pressure. This heated water may reach the earth's surface usually emerging in the form of a warm spring (Holmes, 1964). Hot springs are such extraordinary and easily recognisable features that, except for the most remote and uninhabited areas, their existence is generally known to the local people. The conditions leading to ground water emerging at the earth's surface as warm springs are not well understood. The source of heat that heats the water is still a subject of debate (Holmes, 1964)

In general some of these sources have been identified, but which is the most active at any one occurrence can only be confirmed by detailed investigations.

Some hot springs like those of eastern Tibet, may contain a mixture of meteoric water with juvenile emanations and hot connate water ascending from underlying zones of metamorphism and granitization. Most hot springs however, result from the emergence of ground waters, mainly of meteoric origin, which have passed through volcanic rocks. Those waters would also have had contact with hot volcanic gases or other hot emanations before reaching the earth's surface (Holmes, 1964).

A number of occurrences of hot springs have been recorded over the earth's surface some of which could be large enough to generate hydrothermal energy (power). The power generated could be transmitted to far-off centres of populations. For example, a number of hot springs are known within the Sperkhios Valley, Greece. Their origin is associated with young tectonic movements of the Sperkhios graben and is closely related to the karstic limestone and dolomite massifs of the southern mountainous regions (Dounas *et al.*, 1972). In some regions, the water that emerges from hot springs is largely ground water that has been heated in contact with hot rocks and forced to the earth surface. This could be water that has been originally held in rising bodies of magma.

A region of deep, hot ground water beneath the Imperial Valley of Southern California was investigated in great detail (Ellis, 1975). The area involved measures 5200km^2 and extends over the border into Mexico in the Mexican valley. The region is tectonically active and has been interpreted as a zone of crustal spreading in which the lithospheric plate is being fractured. A number of hot springs are found within the region. The rising basalt magma, usually found in active spreading zones such as in Iceland in the North Atlantic, may be responsible for the source of heat in the springs (Ellis, 1975).

As described in the preceding paragraphs, a number of sources for the source of heat in hot springs are possible. In some areas, the intrusion of magma has been sufficiently

recent that solid igneous rock of a batholith is still hot at a depth of 2 to 5km. At this depth, the rock is strongly compressed and contains little or no ground water. The rocks in these types of regions may attain temperatures as great as 300°C. If there is any existing water within the vicinity, then these high temperatures could supply enormous quantity of heat which will heat the water. The water may reach the earth's surface as hot springs.

In some cases, heat due to the decay of radioelements is enough to explain the source of heat for hot springs. It has been established that the heat produced by radioactive disintegration probably represents the most important factor in the establishment of thermal conditions within the earth (Birch, 1954). Heat production due to some radioactive disintegration is given in Table 1 in section 2.2. As far as significant contributions to the heat of the earth are concerned, the number of radioactive elements to be considered are relatively few (Birch, 1954) Two isotopes of uranium, U^{238} and U^{235} and Thorium, Th^{232} have long half-lives and are distributed within the rocks of the earth's crust. Potassium, K^{40}, is also important in this regard and was even more important in past geological time when it was more abundant. Some hot spring waters like those of Nevada indicates varying abundances of Ra^{226} and Rn^{222} in spring systems where $CaCo_3$ is the predominant material being deposited. The radioactivity of the radioelements could be responsible for the source of heat which heats the water in the Nevada spring.

1.2 The Wikki Warm Spring

The Wikki warm spring is a feature within the Yankari National Park and is a tourist delight for swimming. Yankari Game Reserve itself is located within the Benue Trough and like in other places within the Trough, the water is contained with a thin layer (generally only several hundred metres in thickness) "floating" upon a layer of heavier saline water. Examples of these are famous Kaena and Awe Salt Springs in western part of Benue Trough closer to Yankari Game Reserve. The Wikki warm spring is about 1.9m deep and 13m wide and flows at the rate of 21 000 000 litres daily (Ike *et al.*, 1988). Its temperature of about 31.1°C, which remains constant all year round is higher than the annual temperature of the surrounding which is 26°C. This temperature of 31.1°C is responsible for the belief that the spring is of the Ascending type (Ike *et al.*, 1988).

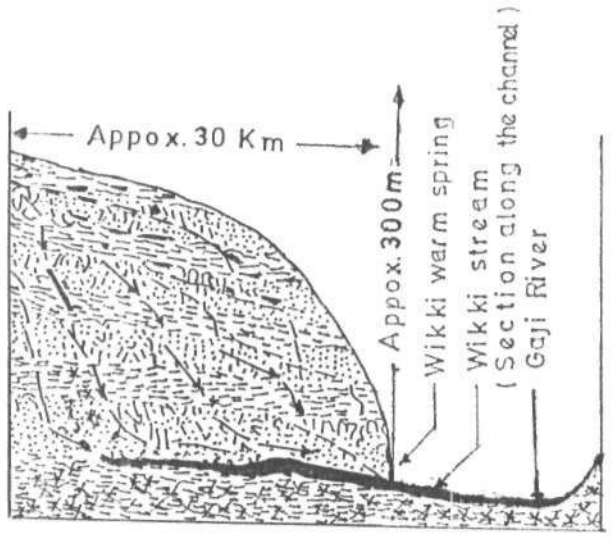
The Wikki warm spring belongs to the fifty largest springs in the world and is the largest in Nigeria (Ike *et al.*, 1988). The largest spring in the world is the Fontaine de Vancluse in France which yields up to 9 763 000 000 litres daily (Ike *et al.*, 1988). In addition to the Wikki warm spring, there are three other warm springs in the Yankari Game Reserve. These are the Gwana warm spring, the Dilimi warm spring and the Mawulgo warm spring. These springs form a "spring line" along the bank of the River Gaji but are not likely to be controlled by faulting or fractures. They are rather connected with the base of the coarse porous sandstone

sequence which rests on a semi-permeable clay unit at the bottom of the River Gaji Valley (Figs. 1.1 and 1.2). The "cold" Tungan Maliki spring discharges water from a horizon near the ground surface and its temperature is close to the annual mean air temperature in the Game Reserve (Ike *et al.*, 1988).

1.2.1 Location of the Area

The Yankari National Park, Bauchi State, Nigeria was established in 1956 and was opened to the public in 1962. The game reserve lies between latitudes 10°45 and 11°15N and longitude 9°50 and 10°50E. It covers an area of 2244km^2. The whole area falls within Duguri, Pali and Gwana districts of Alkaleri Local Government Area of Bauchi State. From Bauchi, access to the reserve is by Bauchi-Gombe road for a distance of 38km to Dindima on the East bank of the Gongola River; then by the Dindima-Gar-Mainamaji road for a distance of 30km to the Mainamaji base camp at the North-Western corner of the Reserve. From the base camp, another distance of 42km takes you to the visitors' camp at Wikki, the location of the Warm Spring.

The game Reserve lies between the Guinea Savanna Vegetation zone with an average annual rainfall of 1100mm. Within the Game Reserve there are a number of rivers. The most prominent is the Gaji River which originated from the Gongola River and runs from north to south across the centre of the Reserve (Figs. 1.3 and 1.4). At the northern part of



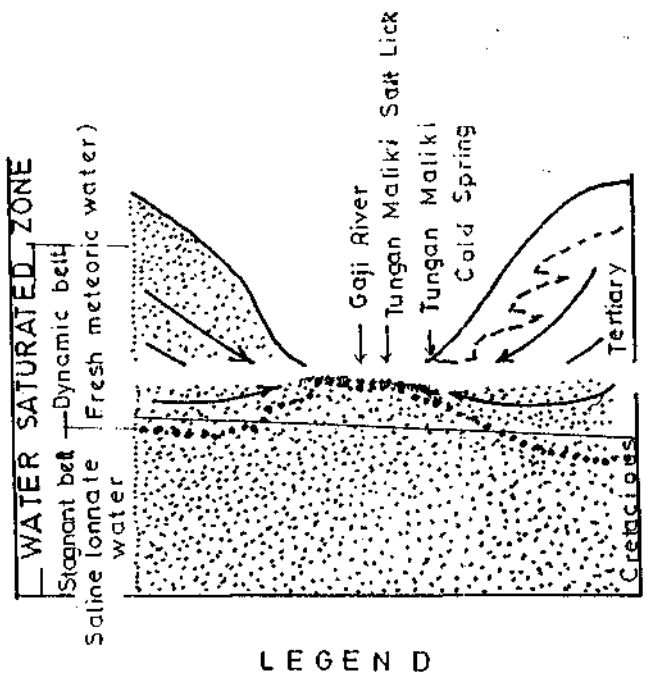
KEY

Sandstones Siltstones, Claystones

Water Body Water Table Direction of ground water flow

FIG.1.1 : SCHEMATIC CROSS-SECTION THROUGH WIKKI WARM SPRING.

(Source; Ike et al, 1988)



LEGEND

Interpondded sandstones, siltstones, mud stones and claystones.

Boundary between Tertiary and Cretaceous deposits

Boundary between fresh meteoric water in the dynamic belt and saline connate water in the stagnant belt of the water saturated zone

Water table and direction of ground flow

FIG. 12 SCHEMATIC CROSS SECTION THROUGH TUNGAN MALIKI SALT LICK AND COLD SPRING

(After Ike et al, 1985)

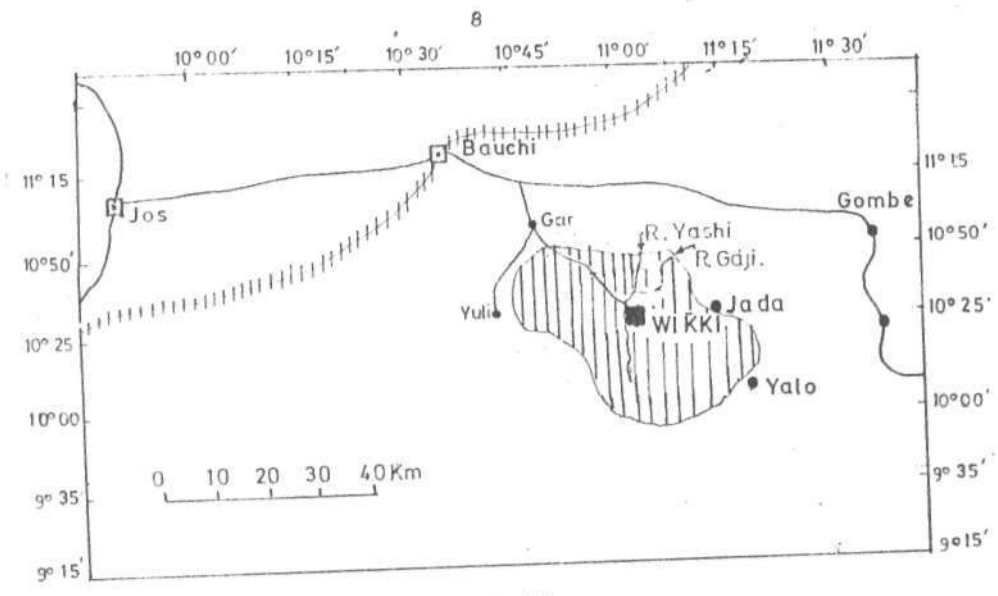
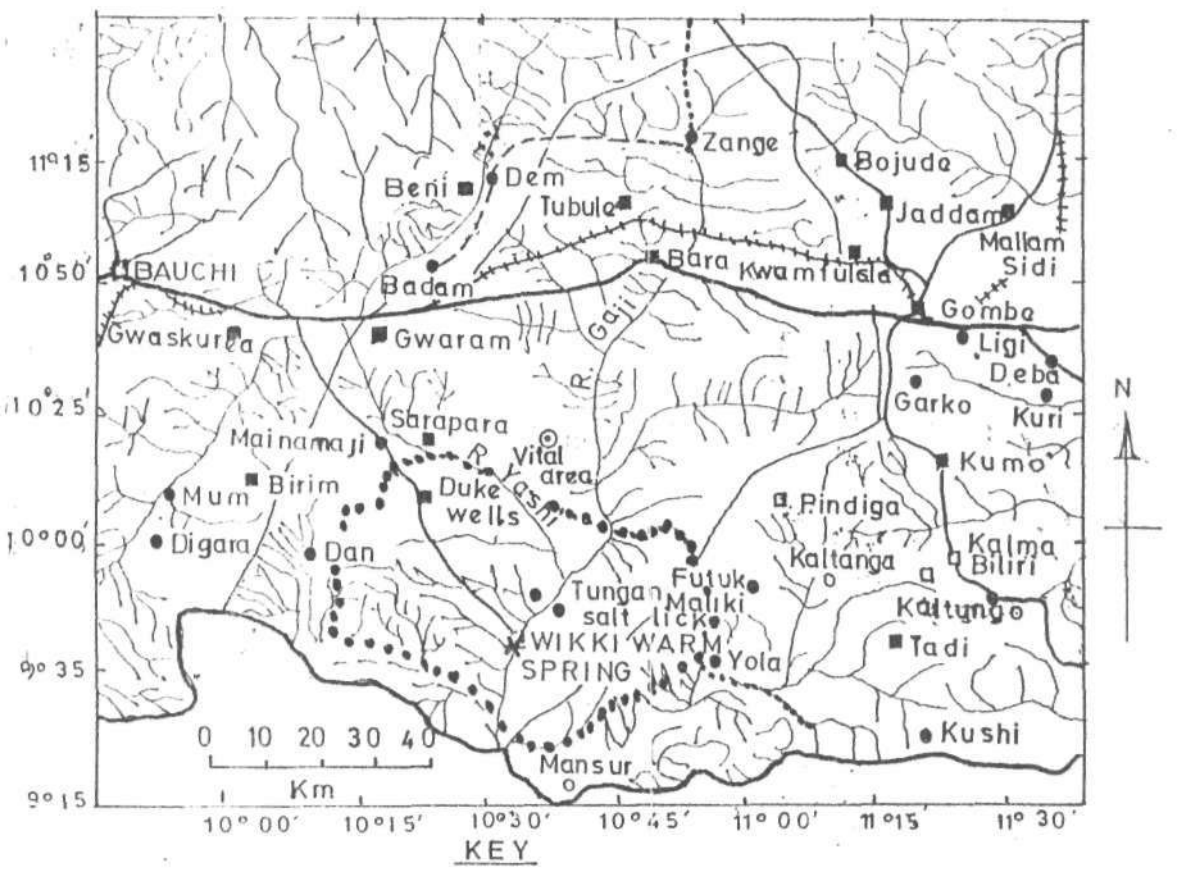


FIG.1·3 LOCATION MAP OF WIKKI WARM SPRING AT YANKARI GAME RESERVE.



KEY

✳ WIKKI WARM SPRING — Rivers & Streams ⊙ Vital area

Game reserve boundary ■ Town • Village ++++ Rail

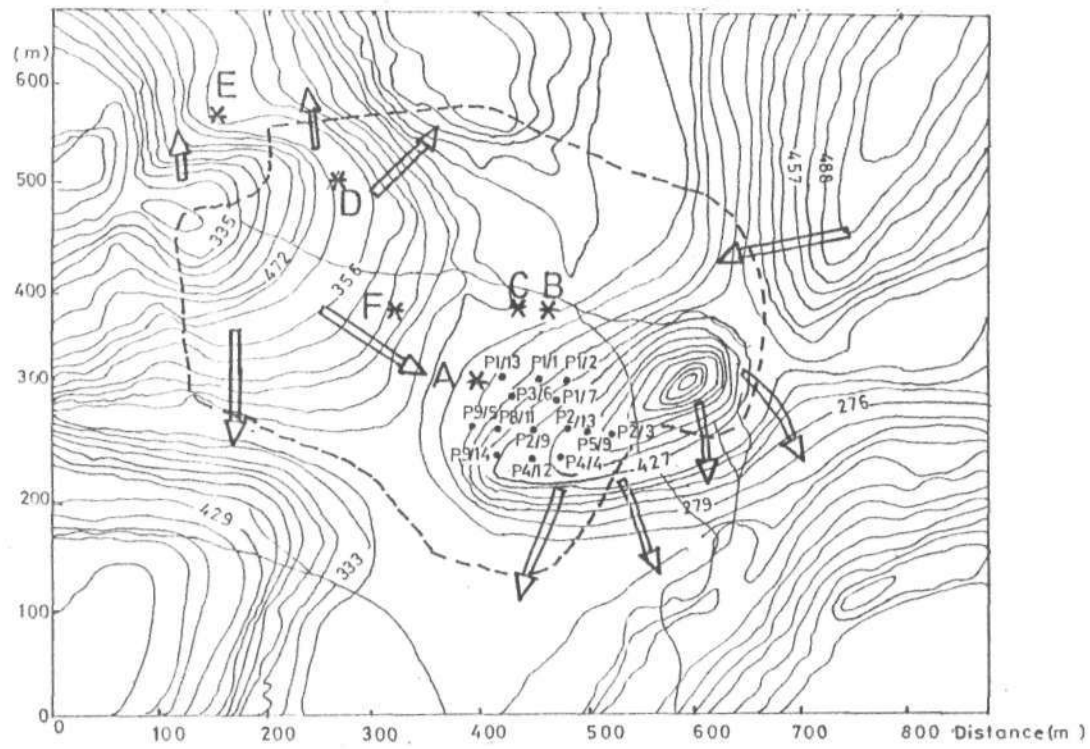
—— Road ----- Path

FIG.1.4 LOCATION OF THE YANKARI GAME RESERVE WITHIN VITAL AREAS FOR THE SURFACE WATER PROTECTION.
(After Ike, et al, 1988)

the river, it is joined by the River Yashi from the west. The flow of the river is supplemented by a number of hot springs.

The Yankari National Park has a number of interesting features, including warm springs. At the visitors' camp at Wikki, there is a warm spring which provides excellent bathing facilities. The Wikki Warm Spring which is the area of study in this work, is situated in a gorge below the Wikki camp and cemented stair-way lead down from the camp to the warm spring. The water flows out of a cave at the foot of a sandstone cliff. The mouth of the cave is several metres wide and, it is located some metres below the water level. The water in the spring is always at a constant temperature of 31.1°C.

Yankari National Water Company is located not far from the entrance to the Reserve. The location of the Company tapping water so close to the spring was a source of concern to the general public. It was then feared that the Company will intercept water recharging the famous Wikki Spring, reducing in this way the flow of the spring. A thorough hydrogeological investigation was carried out, the result of which dispels such fears (Ike *et al.*, 1988). Fig. 1.5 shows a hydrogeological map of Yankari Game Reserve. In this Figure is shown the direction of flow of ground water in the area. Water to the Wikki Warm Spring marked "A" in Fig. 1.5 flows in opposite direction to the point where Yankari National Water Company Supply (marked "E" in Fig.1.5) taps its water. The Company is thus not-tapping the water flowing to the



L E G E N D

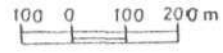
Game Reserve boundary — River and Streams — o Springs and wells — Direction of ground water flow.

—427— Peak of the rainy-season ground water table contours in metres above mean sea level.

A = Wikki warm spring B = Tungan Maliki cold spring and Tungan Maliki Salt Lick C = Mawulgo warm spring

D = Duke wells E = Yankari water company bore holes F = Water holes • VES Points

Fig 1·5 Map showing ground water table at peak of the wet season and directions of ground water flow for the Yankari game reserve (After Ike et al, 1985)



Wikki Warm Spring. It was therefore concluded that the Company does not pose any threat to the Wikki Warm Spring and the Reserve as earlier feared.

1.2.2 Geology of the Yankari Area

The Yankari Game Reserve is located within the Upper Benue Trough. This forms part of the Benue Basin which links up with the Chad Basin in the north and extends southwards to the Anambra Basin (Fargher, 1961). The whole of the reserve is located on sedimentary rocks probably of Cretaceous and Tertiary Ages. The area north-west of River Gaji, that is, between Wikki and Mainamaji, is underlain by sandstones with crystalline rocks of the Precambrian. Basement rocks outcrop to the west and extend to about half a kilometre north-west of the entrance to the reserve. Along the 42km track and the entrance to the Wikki there are only 4 or 5 small rock exposures. They are mostly composed of medium grained, dark red sandstone; the largest exposure is about 12km North-west of Wikki, that is, half way along the new 25km stretch of track from Wikki (Fargher, 1961).

The Wikki Spring itself is located about half a kilometre West of River Gaji on the edge of a small escarpment of sandstone. The escarpment is about 60m high and runs parallel to the River Gaji. The escarpment is probably the end of Tertiary aged sandstones and the rocks Eastward from its base are Cretaceous in age being composed of shells and sandstones (Fargher, 1961).

The escarpment is made up of flat-lying coarse, medium and fine-grained red and white sandstones (Fig. 1.6). The Wikki Warm Spring has its source at the base of a massive current bedded, red sandstone bed, 9m thick. This bed itself is overlain by about 18m thick of poorly exposed rock. The water comes out in a stream 13m wide, 1.9m deep and flows into the River Gaji. The water is crystal clear and fresh, and emerges with high pressure and flows with high speed. 8km North east-wards from the Spring, along the scarp at the water head, the rocks are well exposed. Here a 9m thick bed of sandstone that looks identical to the one at Wikki, forms the top of the escarpment. It is underlain by about 0.6m to 0.9m of shelly rock (Fargher, 1961). At the fine grained sandstone-shale junction, there are several seepages. It seems that this is the extension of the 9m band sandstone at Wikki and the impervious subsurface water running into the sediments from the basement complex rocks many kilometres to the west may be exerting a head in the sandstone causing the swift flow of water at Wikki. The impervious band may correspond to the junction between Tertiary and Cretaceous rocks. That is, the water may be oozing out along the unconformity (Fargher, 1961).

1.3 Aims and Objectives of the Study

The aim of this study is an attempt to identify the origin of the source of heat which heats the water at the Wikki Warm Spring. The investigation is also concerned with the point where this heating takes place, that is, whether

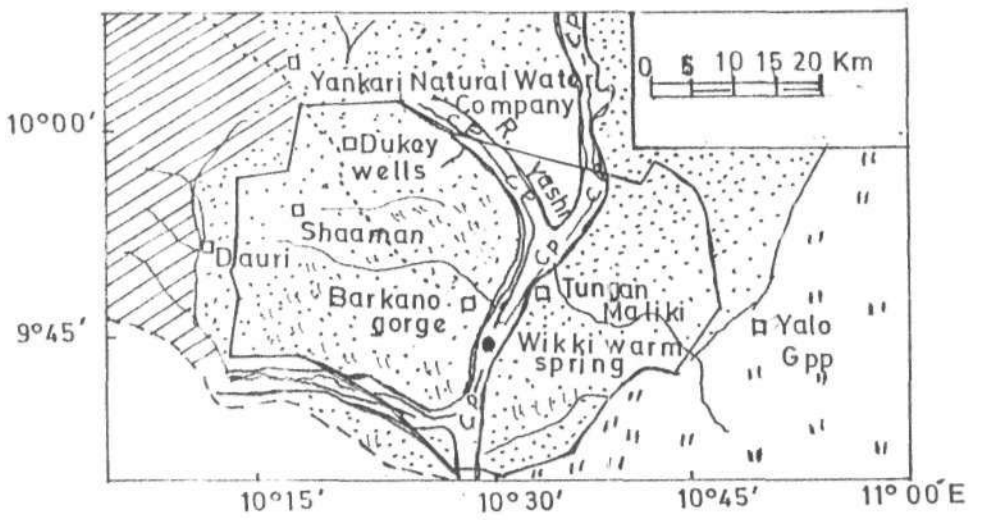


FIG.1·6 GEOLOGICAL MAP OF YANKARI GAME RESERVE.
(After Ike et al, 1985).

the water is heated in the immediate vicinity of the Spring or at some distant point.

Both resistivity and radiometric methods were employed in this work to investigate the source of heat of the Wikki Warm Spring. Resistivity studies have been used to explore for underground thermal waters. Such studies show that limited extent of resistivity anomalies (that is, of low apparent resistivities) always indicate that near surface thermal waters exist. In a study of the springs in the Sperkhios Valley, Greece, it was found that low apparent resistivities were mostly associated with geothermal springs (Dounas *et al.*, 1972). The thermal waters over which these low resistivities are recorded may be contained in altered and intensely fractured rocks. Radiometric studies have also been used to explore for underground thermal waters. These studies show that high radioactivity in an area are responsible for the source of heating the water in such an area. Gamma-ray spectrometry was therefore used to map the distribution of ^{40}K, ^{238}U and ^{232}Th which are a source of heat in the earth crust. These two methods, resistivity survey and radioactivity measurements were used to investigate the source of heat in the Wikki Warm Spring.

The results of the investigation are given in Chapter 4 and fully discussed in Section 5.1. Based on the results of this investigation, a number of suggestions are given in Section 5.2.

Geothermal regions store enormous amount of energy which can be exploited for the generation of electricity. It is in this regard that these studies become very relevant.

Chapter Two

GEOTHERMAL ENERGY

2.1 The Nature and Occurrence of Geothermal Energy

In certain regions of the earth, high temperatures occur which may sometimes be as much as a hundred times the normal. These high temperature gradients are indicative of large heat sources underground. It is the heat in these regions that is termed geothermal energy (McKenzie, 1968). Such thermal regions are usually, but not always closely associated with volcanic activity and earthquakes (Bullard, 1968), that it was believed that volcanism forms the source of heat in these regions. The world's principal earthquake zones are easily accurately known (e.g. Bullard, 1968 showed that majority of these earthquakes occurred in clearly defined belts, or zones of comparatively narrow width). The most important of these zones, which also contain a great number of active and extinct volcanoes, more or less follows the periphery of the Pacific Ocean. Another important zone runs along the middle of the Atlantic Ocean with the Middle East into Tibet. Yet another important zone more or less follows the direction of the Great African Rift and the Red sea. All these zones are interconnected with one another, except for a small isolated zone centred on the Hawaian Islands.

Geothermal areas generally tend to lie within these earthquake belts, though not necessarily close to volcanoes. For instance, Larderello in Italy and the Geysers in

California, two of the most famous geothermal fields, lie at considerable distances from the nearest volcanoes. Thermal areas are also known which occur outside the earthquake zones e.g. in Kenya, Hungary and various parts of the Soviet Union.

The earth is a great reservoir of heat energy but most of its heat is buried too deeply or spread too diffusely to be felt at the surface. That the earth is a great heat engine becomes apparent only during great events such as volcanic eruption, when material at temperatures upward of 800°C is emitted at the surface and during earthquakes. Hot springs, geysers and fumaroles are other manifestation of the earth's heat. Geothermal energy which manifest itself in the form of geysers, fumaroles and pools of boiling mud was regarded merely as an interesting freak of nature, a tourist attraction. These energy sources are however now being gradually developed and put into use in many applications.

At the surface of the earth, a great variety of rock is found; sometimes sediments, such as clays, sandstones or limestones; and sometimes lava from basalts which have been poured out from volcanoes. The sediments are of great importance for geology as they contain most of the oil and a major part of other mineral resources of the earth. Beneath the sediments of the continents, there lies a basement composed predominantly of granite. Some granites have been formed by the freezing of molten material and some by the metamorphism of sediments by heat and by liquids and gases rising from below (Bullard, 1968).

The actual source of the heat in geothermal systems is now almost universally believed to be radioactivity, mostly within the crustal rocks, while the theory of "continental drift" offers an interesting and plausible explanation of the broad confinement of earthquakes to certain clearly observable zones. It is in these zones that crustal weaknesses enable deep seated heat to rise nearer to the surface of the earth.

It is not surprising that man has sought to make use of this heat. In ancient times the Romans, and in modern times the Icelanders, Japanese, Turks and others have used it for baths and for space heating. The Maoris in New Zealand too have exploited natural heat for domestic needs. One of the more interesting sights in New Zealand is a Maori village near Roturua, in North Island, where one may see a fisherman catch fish from his trout and drop it into a nearby pool of boiling water to cook it. A few yards away may be seen his wife administering a geothermal bath to the baby, while his daughter is doing the household laundry and the potatoes are cooking over a fumarole.

At Lardello in Tuscany, the Italians have been extracting boric acid from steam jets ever since the 18th century and it was here that electricity was first generated from geothermal heat. The amount of power now being generated for public electricity supply purposes in various parts of the world from geothermal steam is over 700 mw (Lee, 1965).

The ability to transmit electric power over long distances to some extent immunises geothermal energy against these disadvantages of location, as power may be generated at the field and transmitted to far-off centres of population. It is probable that power generation will remain the most important application of geothermal energy in the near future. It is used extensively for district heating, particularly in Iceland, and for raising "forced" vegetables and flowers in heated glass green houses in Iceland and parts of the U.S.S.R., where the climate is too harsh to support normal husbandry. It is also used for heat-intensive industries for example, for paper making in New Zealand and for the recovery and processing of diatomite in Iceland.

2.2 Source Heat in Warm Springs

Various theories and "models" have been advanced to account for the origin of geothermal heat and the mechanism of its upward transfer towards the surface of the earth. It is found that a heat flow of 1.2μ cal/cm^{2}s is not a large flux of heat by the standards of the kitchen or the factory. In geologic settings, however, this is impressive owing to the long period over which it is maintained. The earth is more than 4,500 million years old and of this about 3,500 million years are represented by rocks near the present surface. Taking an average heat conductivities of rocks and assuming conduction to be the major heat transfer mechanism in the earth, then in 1,000 million years a heat flow of 1.2μ cal/cm^{2}s implies a total heat conduction of 4×10^{10} cal/cm^2

(Bullard, 1969). If this were to be produced by the combustion of coal alone, it will require the consumption of 4 tons under each square centimetre of the earth's surface - that is the complete burning of a layer 20km thick. Clearly the observed heat on earth's surface cannot be produced by burning coal or indeed by any chemical reaction near the surface. Therefore some other sources need to be invoked to explain the observed flow over geological time-spans.

Some of the heat heating waters observed in warm springs may come from the cooling of the earth. In this process it is believed that when the earth was formed, it was molten and hot. However, the initial temperature of the earth is unknown, there is some doubt about how large a part of this heat may be. Lord Kelvin in 1872 showed that if heat is transferred to the surface by conduction in solid earth and if the earth was initially at the melting point, then after 100 million years, the original heat would be only a small fraction of the heat now observed.

Other possible sources of heat within the earth include heat from the cooling of hot magma, volcanism, heat generated during metamorphism, granitization and radioactivity. Of these, the most outstanding one is the heat due to radioactivity of rocks. All rocks contain some amounts of radioactive elements. The most important of these elements are uranium, thorium and potassium. Uranium has two long lived isotopes; ^{238}U which decay to lead (^{206}Pb) through a long series of intermediaries and ^{235}U which decays to ^{207}Pb.

Thorium has a single long-lived isotope ^{232}Th, which also decays through many intermediaries to lead (^{208}Pb). The rare isotope of potassium, ^{40}K, decays by two roots - one to ^{40}Ca (calcium) and the other to ^{40}Ar (argon). The half-lives and heat production of these isotopes are summarised in Table 1. The amount of heat generated in different rock types are also given in Table 2.

From the figures in Table 2 it is clear that heat from radioactivity is more than enough to account for the observed heat flow in geothermal areas. Infact since a thickness of 14 km of granite would produce a flow of 1μ cal/cm^{2}s (Bullard, 1969), it is necessary to assume that the rocks below the crust are much less radioactive than crustal rocks; otherwise the heat flow would be much greater than is observed. Such an assumption is quite reasonable since the more basic rocks are much less radioactive than the granite (Bullard, 1969).

There is some direct evidence that the heat flow through the continental shield areas is due to the radioactivity in the crust. It has been found that the heat flow is greater in areas of high radioactivity than it is in areas where rocks are less radioactive (Roy *et al.*, 1968).

Knowing the heat flow at the surface, it is possible to make a rough estimate of temperatures all through the crust and in the upper part of the mantle, the main uncertainty being the distribution of radioactivity at depth. In the

Table 1: Heat productivities of radioactive elements (after Birch, 1954).

Isotope	Half-life x 10^9yrs	Proportion of Isotope %	Heat Generation (cal/yr)	
^{238}U	4.50	99.27	0.70	
^{235}U	0.71	0.72	0.03	
^{232}Th	13.90	100.00	0.20	}0.73
^{40}K	1.31	0.012	27×10^{-6}	

Table 2: Typical heat production in rocks (Bullard, 1969)

Rock type	Concentration		Heat Production (Ucal/gyr)				
	U(ppm)	Th(ppm)	K(%)	U	Th	K	Total
Granite	4.7	2.0	3.4	3.4	4.0	0.9	8.3
Basalt	0.6	2.7	0.8	0.44	0.54	0.23	1.31
Peridotite	0.016	0.004	.0012	.012	.001	.0003	.0133

continental area where the heat flow is 1.2μ cal/cm^{2}s, if half of this heat comes from a crust 35km thick with a conductivity of 0.005cal/cm°C then the temperature at the Moho, the boundary between the crust and the mantle would be 630°C. Obviously there is a great uncertainty, but temperature in the range 500 to 700°C seems reasonable. If the material below the Moho were static and the heat were transported by conduction, the gradient just below the Moho would be 12°C/km and a temperature of about 1400°C would be reached at a depth of 100km. The melting point increases with depth, but it seems likely that the temperature increases more rapidly and that the material of the mantle is near its melting point at depths of about 100km. At greater depths the increase of melting point may exceed the rise in temperature and the material is probably in less danger of melting. The approach to melting at depths around 100km is perhaps the cause of a slight decrease which is found in the velocity of elastic waves in this region (Bullard, 1969).

The heat of the earth's interior is one of the most immense energy resources available to Man. The energy resource is far greater than the energy available if all the Uranium and Thorium in the earth's crust were employed in breeder reactions (Bullard, 1969).But more important than the sheer size of the resource are the extent of the resource that can be developed with present technology and at an acceptable cost.

A large part of the water and steam emerging in geothermally active areas is not actually derived from deep seated molten rock but from the circulation of ground water. Most basalts are full of joints and cracks and it is easy for rain water to penetrate deeply and reach the hot materials, here it is itself heated and caused to rise, taking with it dissolved materials. When it reaches the surface it may emerge as steam or hot water or a mixture of the two.

As molten rock approaches the surface of the earth, complex series of processes take place. The pressure will be reduced, gases and liquids held in solution are released, the temperature will fall and crystallization will begin (Jeffreys, 1970). Then lava which is a complex mixture of oxides and silicates is formed. The lava is capable of producing many different solid substances depending on the pressure, the temperature and the amount of water and other volatiles present. In general, the first substance to crystallize will be those with the highest melting point, these will be basic rocks without free quartz (Bullard, 1969). The crystals will be denser than the liquid and will tend to settle to the bottom of the molten material; how far they are able to do so will depend on the size of the crystals, the viscosity of the melt and the geometry of the cavity in which it is contained. The composition of both the melt and of the separating crystals may also be affected by eating away and solution of materials from the walls of the cavity. Heat will be transferred continuously throughout this

process of magmatism. In some regions, heat is generated in layers of liquid, the temperature rises and heat flows out by thermal convection.

2.3 Heat Transfer in the Earth

The enormous heat resources within the bowels of the earth are transferred to the earth's surface. There are varieties of ways in which these transfers take place. These include convection, conduction and radiation.

Heat is continually being generated by the decay of radioactive elements and this is likely to be the ultimate source of heat (energy) as we see displayed at the surface of the earth. If heat is generated in a layer of liquid the temperature rises and flows out by thermal convection. This usually involves motion of the material; and if the rate of heat generation continues and exceeds a limit known as adiabatic gradient, the liquid becomes more unstable and the motion becomes faster. Hot liquid then rises towards the surface where it cools and sinks again. Such motion is called thermal convection; once it starts, most of the heat is transported thereby and conduction is unimportant except in a layer near the surface (Roy *et al.*, 1968).

The adiabatic gradient can be expressed as

$$\frac{g\alpha T}{C}$$

where α is the coefficient of expansion of the material, T is the absolute temperature, g is the acceleration of gravity and C is the specific heat. The coefficient of expansion of a rock depend to a large extent on conditions that the rock has a high or low pressure. For example, the coefficient of expansion of a rock in the mantle will be less than it would be at atmospheric pressure. Both from theoretical calculations and experimental results carried out at high pressures, average rock coefficient of expansion have been estimated at about 10^{-6}/°C (Bullard, 1968). With this value, the adiabatic gradient is about 1°C/km which is certainly less than the temperature gradient in the mantle if it were static and that the heat is brought up by convection. It is therefore possible to expect both convective and conductive motions in the mantle which is a function of pressure.

2.4 Geothermal Energy Resources

Geothermal resources are some of the natural heat of the earth's crust. The economics of these resource, just like any other resource, is dependent on its abundance and viability of its exploitation. It becomes economically significant only where it is concentrated into restricted volumes in a manner analogous to the concentration of valuable metals in ore deposits or of oil and gas in commercial reservoirs (Jim *et al.*, 1971). Geothermal resources have three major components; a heat source, a reservoir and a means to transfer the heat in the system. Geothermal energy can be visualised in to

three basic groups. These are hydrothermal, radiogenic and hot rock resources.

Hydrothermal energy resources are characterised by natural thermal waters and the Wikki Warm Spring fall within this class. As shown in Table 3, there are four types of hydrothermal energy resources which include convective hydrothermal resource with vapour dominated and hot water dominated. Other hydrothermal resources include those within sedimentary basin/region aquifers and hot fluid under pressure that is greater than hydrostatic. Only hydrothermal energy resources have been developed to some extent, because the process of developing the others is still uneconomical.

Convective hydrothermal resources are geothermal resources in which the earth's heat is actively carried upward by circulation of naturally occurring hot water or steam. Underlying the higher temperature regions in some of these resources is presumably a body of molten or recently solidified rock (Batchelor, 1982).

Geopressured resources consists of deeply buried fluids contained in permeable sedimentary rock warmed in a normal or anomalous geothermal gradient by their great depth of burial. These fluids are tightly confined by surrounding impermeable rock and are thus subjected to pressures that is much greater than hydrostatic (Wallace *et al.*, 1979). Typical example of these are in the U.S. Gulf Coast area where geopressured fluids record temperatures up to 150°C and even

higher where they contain methane. From the geopressured resources, three forms of energy may be available; (i) heat, (ii) mechanical energy derived from the high well-head pressure and (iii) recoverable methane. Development of these resources was assessed by a research programme co-ordinated by the Idaho National Engineering Laboratory for the U.S. Department of Energy (Wallace *et al.*, 1979). Results of these research programmes are however not yet fully assessed.

Table 3: Geothermal resource classification (White *et al.*, 1975).

Resource Type	Temperature Characteristics
1. Hydrothermal resource (convective)	
(a) Vapour dominated	about 240°C
(b) Hot water dominated	about 30°C to 350°C
(c) Sedimentary basin/region aquifers	30°C to about 350°C
(d) Hot fluid under pressure that is greater than hydrostatic	90°C to about 200°C
2. Radiogenic (heat generated by radioactive decay)	30°C to about 150°C
3. Hot rock resources	
(a) Partly molten	higher than 600°C
(b) Solidified (hot dry rock)	90°C to 650°C

Radiogenic geothermal resources do occur in some part of the world. A typical example is the Eastern U.S. where the coastal plain is blanketed by a layer of thermal insulating sediments (Costain *et al.*, 1980). It is believed that the

granitic intrusions having enhanced heat production from radioactive decay occur in places beneath these sediments.

Hot rock resources, comprise those which have little or no natural hydrothermal convection, and the resource may be molten or partly molten. The feasibility and economics of extraction of heat from hot, dry rock is presently the subject of a co-operative research effort among the U.S., the Federal Republic of Germany and Japan. The research is centred at the U.S. Department of Energy's Los Alamos Natural Laboratory in New Mexico (Smith *et al.*, 1982). Similar experiments have been carried out in England (Batchelor, 1982). The results of these experiments are however not yet fully assessed. The Wikki warm spring at a constant temperature of 31.1^{0}C is located within a sedimentary basin. It is therefore possible that the source heat is of the radiogenic geothermal resource type. The subject of this study is to determine these types of possibilities. The results are presented in Chapter three and fully discussed in Chapter four.

Chapter Three

RESISTIVITY AND RADIOMETRICS IN GEOTHERMAL RESOURCE EVALUATION

3.1 Resistivity surveys: Principles, techniques and applications

The simplest approach to the theoretical study of resistivity of earth's material is to consider first the case of a completely homogenous isotropic earth (Telford *et al.*, 1975). The resistivity instrument comprise a current source (battery), a current meter, and a voltmeter. These are connected (Figure 3.1) to four electrodes inserted into the ground to make electrical contact.

An equation which gives the potential about a single source of current can be developed from the following two basic considerations:

(i) Ohm's law:

$$\vec{E} = \rho\vec{J} \quad \ldots\ldots\ldots \quad (1)$$

where $\vec{E}$ = the potential gradient

$\vec{J}$ = the current density

ρ = the resistivity of the medium

(ii) the divergence condition

$$\nabla.\vec{J} = 0 \quad \ldots\ldots\ldots \quad (2)$$

The implication of equation 2 is that all the current going in to a chunk of material must leave the other side

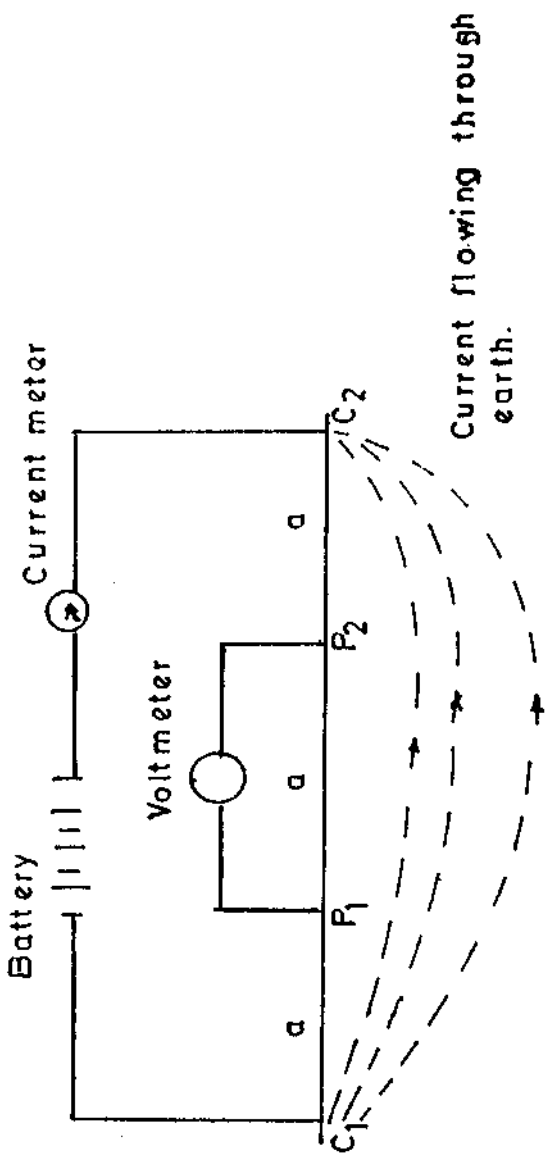


Fig.3·1 Resistivity configuration.

unless there is a source or sink for current within the chunk. The divergence of the current vector must be zero at every place but at the current source.

Combining equations 1 and 2, one obtains the Laplace's equation.

$$\nabla.\bar{J} = \frac{1}{\rho}\nabla.\bar{E} = 0$$

But since E = $-\nabla.U$

$$\nabla.\bar{J} = -\frac{1}{\rho}\nabla^2 U = 0 \quad \ldots\ldots (3)$$

Where U is a scaler potential function defined such that E is its gradient. In spherical polar co-ordinates, the Laplace equation is written as

$$\frac{1}{r^2}\frac{\partial}{\partial r}\left(r^2\frac{\partial u}{\partial r}\right) + \frac{1}{r^2\sin\theta}\frac{\partial}{\partial\theta}\left(\sin\theta\frac{\partial u}{\partial\theta}\right) + \frac{1}{r^2\sin^2\theta}\left(\frac{\partial^2 u}{\partial\phi^2}\right) = 0 \quad \ldots \quad (4)$$

Where r is the radius vector, θ the polar angle and ϕ the azimuth.

If only a single source of current is considered, complete symmetry of current flow with respect to θ and ϕ directions may be assumed.

Hence equation 4 reduces to

$$\frac{1}{r^2}\frac{\partial}{\partial r}\left(r^2\frac{\partial u}{\partial r}\right) = 0$$

and since $r \neq 0$

$$\frac{d}{dr}\left(r^2\frac{du}{dr}\right) = 0 \text{.....(5)}$$

Integrating equation (5) twice gives A and

$$r^2\frac{du}{dr} = A \text{ and } U = -\frac{A}{r} + B$$

where A and B are constants and r is the distance from the current electrode.

Since U = 0 when $r \to \infty$, then B = 0

$\therefore U = -\frac{A}{r}$

If we assume the current to flow at the surface of the earth then

$$I = 2\pi r^2 J = 2\pi r^2 \frac{1}{\rho}\frac{du}{dr} = -\frac{2\pi A}{\rho} \rightarrow A = \frac{I\rho}{2\pi}$$

$$\therefore U = \frac{I\rho}{2\pi r} \text{ .....(6)}$$

If there are several sources of current, as is normally the case, rather than the single source assumed so far, the total potential at any observation point is calculated by adding the potential distribution from each source considered independently. Thus for n current sources, equation 6 becomes

$$U_n = \frac{\rho}{2\pi}\left(\frac{I_1}{r_1} + \frac{I_2}{r_2} + \frac{I_3}{r_3} + \text{.....} + \frac{I_n}{r_n}\right) \text{.....(7)}$$

From equation 6, the resistivity, ρ, can be expressed thus

$$\rho = \frac{U}{I}.2\pi r$$

$$\rho = \frac{U}{I}.K \text{ ..... (8)}$$

where K is the geometrical factor which depends on the type of array used during the field measurement. The geometrical factor, K, is given by

$K = 2\pi a$ ..... (9) for Wenner array, and

$$K = \pi MN\left[\left(\frac{L}{MN}\right)^2 - \frac{1}{4}\right] \text{.....(10) for Schlumberger array.}$$

L is the separation between a current electrode and the centre of the potential electrodes. MN is the separation of potential electrodes, for Schlumberger array.

Using equations 8 and 9 the apparent resistivity, ρ_a, of the earth can therefore be obtained. This is given by:

$$\rho_a = \pi MN\left[\left(\frac{L}{MN}\right)^2 - \frac{1}{4}\right]\frac{U}{I} \text{ for Schlumberger array}$$

$$\rho_a = (2\pi a)\frac{U}{I} \text{ for Wenner array}$$

The choice of method in the resistivity survey depend on the type of surface cover predominant in the area. Since ground resistivity is influenced by temperature (Keller, 1970), the presence of a resistivity anomaly can be indicative of a temperature anomaly.

The important physical property change due to the presence of a hydrothermal system, other than elevated temperature and heat flow is the change in electrical resistivity of the warm fluid (Moscowitz *et al.*, 1977). High temperatures increase ionic mobility and hence increase

conductivity. Ionic conduction in springs also increase with increased amount of certain minerals. Most warm springs are associated with anomalously low resistivity due to one or more of the factors cited above. It is therefore pretty clear that figures of only few ohm-metre should be recorded in hot water reservoir regions as compared with several hundred ohm-metres or more in normal areas.

In deep electrical survey, resistivity measurement techniques involve current injection and voltage measurements by means of separate sets of electrodes in contact with the ground. Most commonly used are the Schlumberger or Wenner electrode arrangements. The two differ only in the disposition of the current and voltage electrodes in a single line.

The method of resistivity profiling or trenching affords one the opportunity of determining the lateral variation in apparent resistivity within a pre-selected depth of the subsurface. The depth of penetration of the current is about equal to the separation for a Wenner array. The method of resistivity sounding or electrical drilling gives detailed information on the vertical succession of various conducting layers their thicknesses and effective resistivities.

Schlumberger profiling is recommended over the area of the surface thermal anomaly and far outside as may be necessary to find apparently normal resistivity values (Van Nostrand *et al.*, 1966). This enables one to know precisely the extent (coverage) of the thermal anomaly. The profiling

is achieved by selecting a fixed electrode spacing and taking successive readings by shifting the whole set of electrodes along the survey line.

In addition to profiling, a number of soundings can be made at selected points to determine the vertical resistivity distribution and possible layering of the earth in the area. The purpose is to determine the depth to the basement or bedrock. A sound is made by keeping the centre of the electrode system at a fixed point and increasing the linear scale of the electrode pattern from low to high values.

Profiling is used for mapping the horizontal variations of the mean resistivity (taken over some chosen range of depths depending on the electrode spacing used) over the survey area. Sounding give the variations of average resistivity as increasing range of depths is included in the average. A plot of apparent resistivity against electrode spacing (sounding curve) can be used to calculate such parameters as thickness and electrical resistivity of the layers of a hypothetical ground from which a model of the ground where the survey was carried out can be produced.

To aid in resistivity interpretation, a supplementary geological survey can be used to provide the approximate thickness and compositions of these layers. If clay, or clay-bearing formation of significant thickness are present in the survey area, these may give low resistivity values which may not be associated with thermal anomalies. A geological study can identify such formations and from which their depth and

thickness can be obtained with reasonable precisions. This information can be of considerable value in interpreting resistivity measurements (Banwell, 1961).

The effective depth of penetration of resistivity profiling and soundings in low resistivity formations can sometimes be seriously limited by a phenomenon called "skin effect". This arises if alternating current or direct current of too short a period is used. D.C. resistivity methods are therefore preferred to A.C. methods owing to the "skin effect" present at large spacings with the methods. But if the equipment available permits only the use of A.C., the optimum depth of penetration should be calculated from the frequency used and the measured resistivity, in order to avoid possible erroneous interpretations of the results. It should also be noted that results can be distorted if the soundings are carried out in a field of limited size, the effect usually being to give an apparent increase of resistivity at maximum spread.

Subject to the above limitations, vertical resistivity sounding was carried out in this study. From the soundings, it was possible to deduce whether the warm water, observed in the Wikki spring gets its source from heating in the immediate vicinity of the spring or some distance away from the spring. In hot or warm water field, the resistivity pattern takes the form of central low, representing the porous reservoir rocks filled with hot water. In a steam field, on the other hand, there would probably be a central

resistivity high, because the reservoir rocks are now filled with steam which has low electrical conductivity; surrounded or underlain by lower resistivity zones containing steam heated ground water and condensate (Banwell *et al.*, 1961).

In principle thus, it is possible to obtain information as to the source of heat in warm springs using resistivity methods. In practice, however, things are not quite straight forward and resistivity alone may not give complete information as to the source of heat in springs. Other geophysical techniques therefore would have to be called into play, in addition to resistivity survey. While resistivity survey can give information that may lead to the type of fluid in the formations, radiometrics can be used to determine the significance of radiogenic heat for the source heat in the warm spring.

For this work, Schlumberger arrays was used to obtain variation of resistivity with depth in the area.

3.1.1 Computation of Apparent Resistivity

The field measurements yield readings of potential difference, V, and current, I, at each station. These must be converted to apparent resistivity.

The quantity, V/I measured by the instrument depends upon the subsurface geology. It will also depend on the spacing and geometry of the four electrodes.

We define a new quantity, ρ_a the apparent resistivity, as that combination of potential, current and electrode

geometrical factors which would equal true resistivity if the earth were made of material of uniform composition (Frischknecht *et al.*, 1966). In effect, we normalise the measurements to uniform earth. Thus, any observed variations in the measurements must be interpreted as deviations from a uniform earth. Such deviations represent the target in resistivity surveys.

The computation of the geometrical factor turns the results out to take the form.

ρ_a = K V/1 ..... (11)

or ρ_a = KR

where K is the electrode configuration.

The specific value of K becomes

Wenner : K = $2\pi a$

Lee : K = $4\pi a$

Schlumberger: $K = \pi MN \left[\left(\frac{1}{MN}\right)^2 - \frac{1}{4}\right]$

The apparent resistivity therefore, serves to normalise out the effect of electrode geometry which will be dependent on the subsurface geology.

3.1.2 Choice of Electrode Arrangements

There are basically two methods in the electrical resistivity surveys. The choice of which method to adapt will depend on the type of information being sought. The two methods are profiling and sounding.

In resistivity sounding, the electrode spacing is changed while maintaining a fixed location for the centre of the electrode spread. In this way, the variation of resistivity with depth is obtained. This in turn will assist in determining the different formations in the area being surveyed. Since depth of investigation increases in general with increasing electrode spacing in this method, it is recommended when the aim is to investigate the variation of resistivity with depth.

In resistivity profiling, the location of the spread is changed while maintaining a fixed electrode spacing. Profiling is used to map the lateral variations of the mean resistivity (taken over some chosen range of depths depending on the electrode spacing used) over the survey area. Since the depth of investigation will remain roughly unchanged from one reading to the next, resistivity profiling will be recommended when the aim is to investigate lateral resistivity variations.

Many electrode configurations have been proposed and used in resistivity survey. Whitely (1973) gave a comprehensive review of about 25 arrays with comments on the advantages and disadvantages of each. While some of the less well known arrangements may offer significant benefits, we will here limit our discussions to only two electrode spreads because they are the ones used in this study. They happen to be the most widely used, their interpretation tools are well developed and they are adequate for most applications to

engineering, ground water and shallow geologic problems (Whitely, 1973).

The two arrangements are shown in Figure 3.2. Symbols C_1 and C_2 refer to the positive and negative current electrode, respectively through which current is injected into the earth. Symbols P_1 and P_2 refer to the electrode pair across which the potential difference is measured. Symbols A, B and MN are equivalent designations used for locations C_1, C_2 and P_1, P_2 respectively.

3.2 Field Procedure in Resistivity

For data collection in the resistivity measurements reported in this work, an ABEM Terrameter Model SAS 300B was used. The instrument is a signal averaging machine with digital readout. The Terrameter determines the resistance, in ohms, of the earth material at the sampling point a number of times depending on the setting chosen by the operator. This may be 1, 2, 4, 16 or even 64 times. After sampling the resistance at a point, the machine automatically displays the average resistance of the ground for the spread. To save time and extend the life of the battery in the instrument, a setting of 4 readings (samples) per station was used throughout the data collection stage. The longer the sampling time, the more accurate the resistivity value measured. If however, the sampling time is long, it consumes time and shortens the life of the battery. Also, the instrument has a varied current input into the ground to suit the prevailing soil condition at any one station. For this work, a current

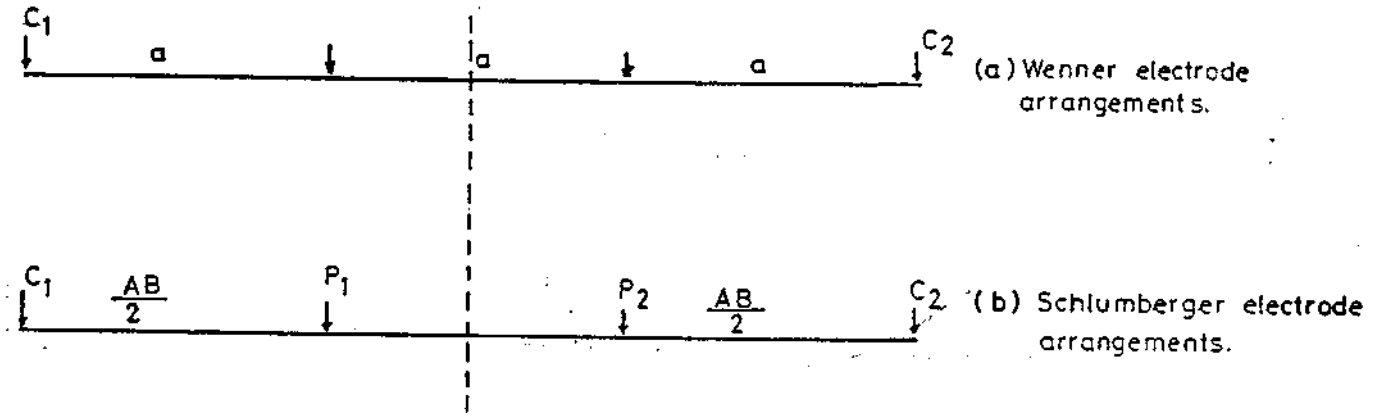


Fig. 3·2 Schematic diagram of the Wenner (a) and Schlumberger (b) arrangements.

value of 5m.. was used for the sounding which is adequate for this survey.

Nine profiles were established for sounding. The maximum AB/2 reached was 250m.

3.3 Field Procedure in Radiometrics

In addition to resistivity measurements, the radioactivity of the Wikki area was also measured to investigate the source of heat of the Wikki warm spring. A DISA 300 four-channel gamma-ray spectrometer was used to carry out this measurement. The same profiles as the ones used for the resistivity measurements were used to carry out the spectrometric measurements. In all the profiles, readings were obtained at stations spaced at 100m interval. At each station, the instrument threshold discriminator was set to take readings from the total count potassium, uranium and thorium windows.

Before taking any reading during the survey, on daily basis spectrometer was allowed to adjust to the temperature of the surrounding for about 5 minutes after taking it out from the container. To take readings at a station, the spectrometer was levelled on the ground. With the instruments in the position, readings for each window were then taken by turning the threshold selector knob to Tc, K, U, and Th corresponding to radioactivity in the total count, potassium, uranium and thorium windows respectively as stated above.

3.3.1 Radioelement Concentration

The procedure for estimating concentration of the three radioelements K, U and Th from spectrometer readings depends on the type of spectrometer used. For a threshold spectrometer, the relationship between the count rate and element concentration is such that the concentration in parts per million (ppm) is directly proportional to the count rate (Doig, 1968). Suppose the count rate in counts per second (c/s) at the Thorium, Uranium and Potassium thresholds are Thc, Uc and Kc respectively, then

eTh (ppm) = k_1 Thc ..... (12)

eU (ppm) = k_2 Uc ..... (13)

%k = k_3 k_c ..... (14)

(Doig, 1968).

where eTh and eU are the thorium and uranium concentration in ppm and %k is the percentage concentration of potassium. k_1, k_2 and k_3 are instrumental constants.

Equations (12), (13) and (14) cannot be used directly to compute the element concentrations because of the background effect. Hence the readings have to be corrected for this effect. If the background readings in c/s in Thorium, Uranium and Potassium thresholds are Th_b, U_b and k_b, then the above equations become

$eTh = k_1(Thc - Th_b)$ ..... (15)

$eU = k_2(Uc - U_b)$ ..... (16)

$\%k = k_3(kc - k_b)$ ..... (17)

(Scintrex, 1973)

And to account for interference of Thorium in the Uranium counts and Thorium and Uranium in the Potassium counts, another constant has to be incorporated into the above equations. These constants, called stripping ratios, come about due to the fact that in detecting potassium, for example, the energy threshold used is 1.46 MeV (Darnely, 1972). That is, all gamma-rays with energy above 1.46 MeV are counted. In this energy range, both gamma-rays emitted by the decay chains of Uranium and Thorium are present, then a mean has to be found for correcting for their contributions. Similarly, for detecting uranium, the threshold of energy used is 1.76 MeV; so the only interference is from the gamma-rays from thorium decay series because gamma-ray energy from the decay of k^{40} peaks at 1.46 MeV. For the estimation of uranium concentration therefore, the effect of gamma-rays from thorium must also be accounted for. But in the detection of Thorium, the energy threshold is set at 2.62 MeV, hence, there is no interference from gamma-rays of either potassium or uranium. Therefore, in terms of the stripping ratios, the concentration equations, become:

$$eTh = k_1(Th_c - Th_b) \quad \ldots\ldots\ldots \quad (18)$$

$$eU = k_2(U_c - U_b) - S_1(Th_c - Th_b) \quad \ldots\ldots\ldots \quad (19)$$

$$\%k = k_3\{(k_c - k_b) - S_2[(U_c - U_b) - S_2(Th_c - Th_b) - S_3(Th_c - Th_b)]\} \ldots (20)$$

where S_1, S_2, and S_3 are the stripping ratios.

Using the above equations, gamma spectrometer measurements were converted to element concentrations. The concentration equations were used to convert the count rates to relative surface concentrations. For the purpose of the

calculation, sensitivity constants and stripping ratios for the spectrometer as given below were used.

k_1 = 7.5 cpm/ppm

k_2 = 20.5 cpm/ppm

k_3 = 154.0 cpm/ppm

S_1 = 0.62

S_2 = 0.68 and

S_3 = 0.83

(Geometrics, 1984)

Inserting these constants, equations (18), (19) and (20) become

$$eTh\ (ppm) = \frac{Th_c - Th_b}{7.5} \quad \ldots\ldots (21)$$

$$eU\ (ppm) = \frac{U_c - U_b - 0.62(Th_c - Th_b)}{20.5} \quad \ldots\ldots (22)$$

$$\%k = \frac{(k_c - k_b) - 0.68(U_c - U_b) - 0.62(Th_c - Th_b)\ 0.83(Th_c - Th_b)}{154.0} \quad \ldots\ldots\ldots (23)$$

The above relations were used to determine equivalent Th, U and k concentrations; eTh, eU and %k respectively. The results obtained are presented in Chapter Four and fully discussed in Chapter Five.

3.4 Problems Encountered in the Field and Limitation of this Work

The initial scope of this work was to cover an area of 2.0km by 2.5km using the two techniques of study. However, the field situation did not allow for that due to quite a number of problems encountered in carrying out the survey. The most important of these problems are:

(a) The Wikki warm spring is located in a somehow deep valley. Access to it from the camp is through cemented stair steps thus neither resistivity nor radiometric survey was possible within the immediate vicinity of the warm spring.

(b) For the fear of wild animals which freely move in the area, moving further away from the camp (built area) was not possible. This means that, the area of coverage of the work was restricted.

(c) Because most of the area of the camp is built-up and the heavy shrubs in the survey area, the area covered by both the electrical resistivity and radiometric survey was also restricted.

These limitations meant that only a very small area was covered, thus limiting the number of data points. Nonetheless, the data obtained and the area covered is sufficient enough for the purpose of this investigation.

Chapter Four

INTERPRETATIONS AND DEDUCTIONS

4.1 Data Processing

For the purpose of calculating the apparent resistivity values, the field measurements which yield readings of potential V and current I at each station and electrode geometrical factors which would give true resistivity if the earth were made of material of uniform composition were taken into consideration. The equations for computing the apparent resistivity are given in Section 3.1.1. The resistivity data collected from the field were processed using equations (11) to obtain the apparent resistivity values ρ_a. The readings of the equipment, while in the field, were in ohms (Ω). This made the computation of the apparent resistivity rather simple.

To determine the apparent resistivity (ρ_a) values, the geometrical factor (k) for each of spread was first calculated using equation (10), taking into account the distances from the electrodes. The factor (k) multiplied by the values of readings obtained from the instrument gave the apparent resistivity values equation (11).

In the case of the sounding data, the apparent resistivity values for each VES point were plotted against the electrode spacing (AB/2) on a log-log graph sheet. This was to acknowledge a general property of the resistivity method; the larger electrode spacings yield information over

a much larger volume of earth; thus a given volume becomes proportionally less important. A second reason is that the widely used method for interpreting resistivity data requires presentation of the resistivity data on logarithmic graph paper.

4.2 Interpretation of the Resistivity Survey Results

The interpretation of data from electrical method involves expressing, in geological terms, the information obtained from the measured apparent resistivity data. For interpretations of data from such surveys, a considerable practical experience with the methods and a good knowledge of the geology of the area is required. For the purpose of this work, all available information on the study area were taken into consideration in the interpretation. For the sake of interpreting the data, the ground in the area was assumed homogeneous and isotropic which implies that the lateral variations in conductance was considered negligible.

The method employed in the interpretation of the data collected as discussed in Chapter Three, involved finding some initial parameters which were subsequently fed into a computer to be used by a program. The computer programme called 'Program Inverse' written by Philip A. Davis of the University of Minnesota and published by Mooney (1980) was used for the analysis. The program essentially produces a model that best fits the observed resistivity values. This was achieved by executing the following steps incorporated in the program.

i. Designing a trial model based on the field results.

ii. Computing the theoretical field curve expected from the trial model.

iii. Comparing the computed resistivity curve with the observed (field) resistivity curve and

iv. Modifying the model, where necessary to improve the match between the computed and the observed data until the best possible fit was obtained.

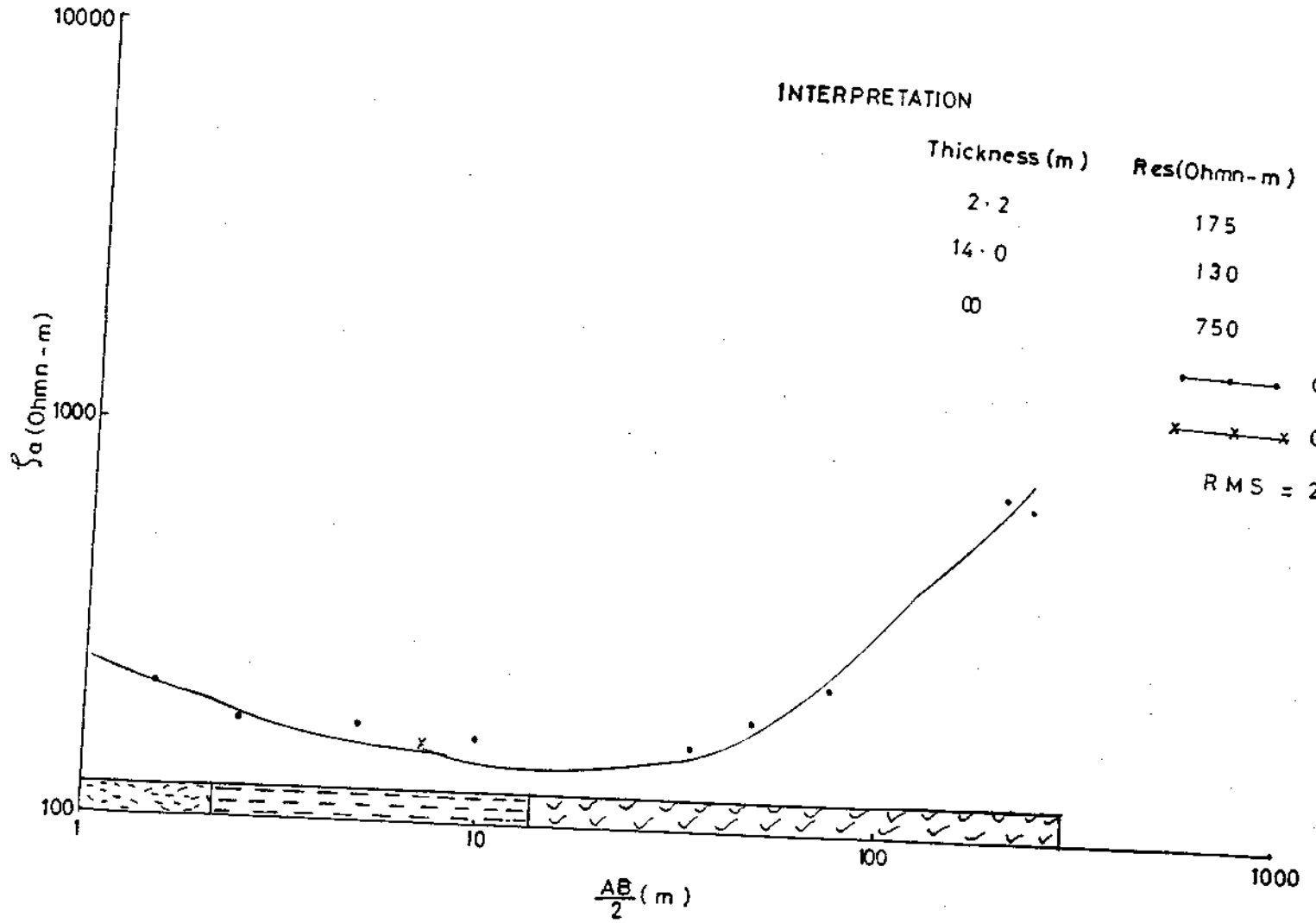
By supplying parameters of the trial model to the program, steps (ii) and (iii) were automatically executed; while step (iv) was carried out only where it was necessary to improve the agreement between the computed and the observed data by altering one or more of the parameters (layer resistivities and/or thicknesses) of the subsurface of the initial or last model. The parameters of the initial model were approximately determined using the conventional method of curve matching (Keller and Frishnecht, 1976; Telford *et al.*, 1976).

The computer program was designed in such a way that it uses the trial model to compute a theoretical apparent resistivity curve. This curve was then compared with the observed field curve and then iteratively modified the initial layer parameters until a 'best fit' between the observed field curve and the computed one was obtained. This iterative process terminates when the process had gone through a specified number of iterations or a given root-mean-square (r.m.s.) value was obtained.

Fig. 4.1 shows the interpretation for the VES P1/1 which illustrates a typical example of the interpreted VES data in this work. Shown in the Figure are the observed resistivity data, computed data for the final model as well as the interpreted geoelectric section and its corresponding resistivity values for the VES point.

The shape of the observed resistivity curve at the VES P1/1 shown in the Fig. 4.1 suggests that three layers of the earth model were sampled beneath that point. Hence, a three-layer model was employed in the interpretation. The computed resistivity values for the final model (h_1 = 2.2m, ρ_1 = 175Ω-m; h_2 = 14.0m, ρ_2 = 130Ω-m; ρ_3 = 750Ω-m) are shown in the Figure by crosses, while the observed resistivity data are shown by dots joined by a smooth curve. At points where dots are not shown, the observed and the theoretical values exactly coincide. Hence, only the "cross" signs are shown at such points. The root-mean-square (r.m.s.) value is the measure of the degree of fit between the computed and the observed data. For this figure, the r.m.s. value is 2.1. The final model suggests that the total depth to the third layer is 16.2m.

All the remaining VES point were interpreted following the same procedure discussed above for VES P1/1. The computed resistivity data for the final model and the interpreted geologic and geoelectric sections for the various VES points are shown in Appendix A.



INTERPRETATION

Thickness (m)	Res(Ohmn-m)	Rock type
2·2	175	Clay, Silt and Mudstones
14·0	130	Sand stones
∞	750	Fresh basement

Observed curve

Computed curve

RMS = 2·1

Fig. 4.1 Resistivity plot for VES **Point** $P_{1/1}$

In interpreting d-c resistivity data, just like any other geophysical method, geoelectric and geologic sections of the various VES points sounded were prepared. Also, resistivity map and isoresistivity maps were prepared by contouring as shown in Figs. 4.2a, 4.2b, 4.3 and 4.4a, 4.4b respectively.

4.2.1 Resistivity Values

Tables 4.1 and 4.2 show the resistivity values for sedimentary rocks and the resistivity values used in deriving the geologic sections in this work respectively.

4.2.2 Geoelectric and Geologic Sections

The interpretation of the geoelectrical sounding data collected is generally not meaningful without some reliable geological control or some data relating to the intrinsic resistivities of the various geoelectric units at several places within the surveyed area (Worthington, 1977). As discussed in Section 3.2, the VES stations in this work were established as shown in Fig. 1.5 labelled P1/1, P1/2, P1/13, P2/3, P3/6, P3/7, P4/4, P4/12, P4/14, P5/9, P6/8, P7/10, P8/11 and P9/5. In Figs. 4.2a, 4.2b are shown the geoelectric and geologic sections derived for the VES points P2/3, P5/9, P6/8, P7/10, P8/11 and P9/5. These sections were based on the interpretations discussed in Section 4.2. The geologic sections were determined using the geoelectric sections and the geological information obtained from the resistivity values of Tables 4.1 and 4.2. Description of the resulting geoelectric and geologic sections are presented below.

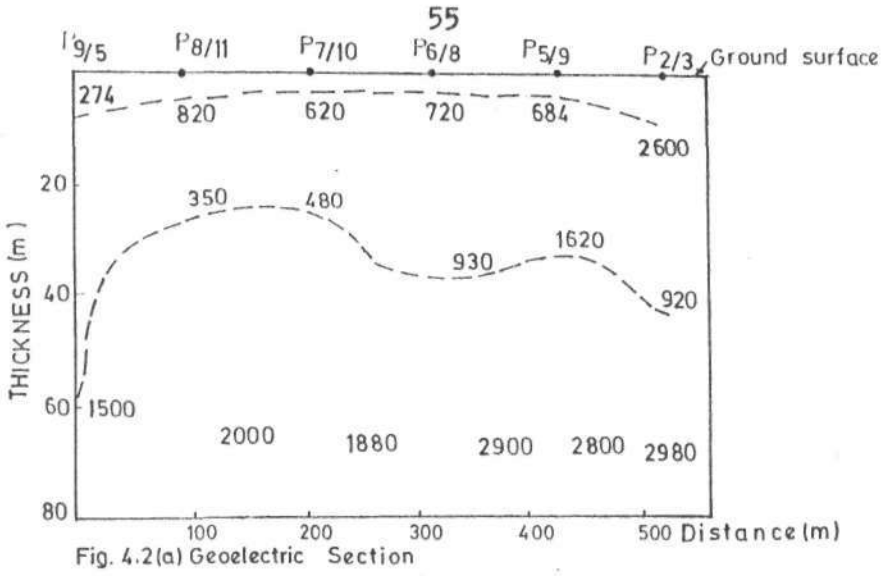


Fig. 4.2(a) Geoelectric Section

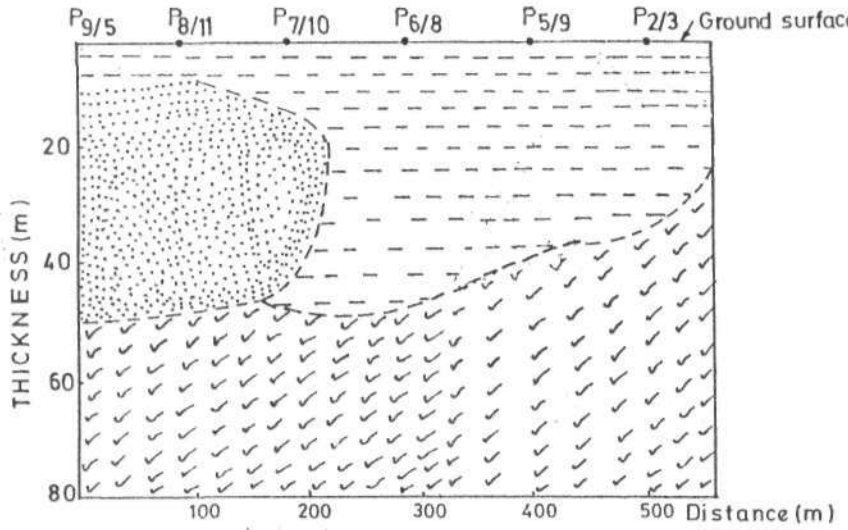


Fig 4.2(b) Geologic Section

LEGEND

Geoelectric and Geologic section | 620 Res. values (Ohm-m) | Very saturated sandstones

Porous sand stones | Fresh basement | • P2/3 VES Point.

Fig. 4.2 Geoelectric and Geologic section for ves points 5, 11, 10, 8, 9 and 3

463493

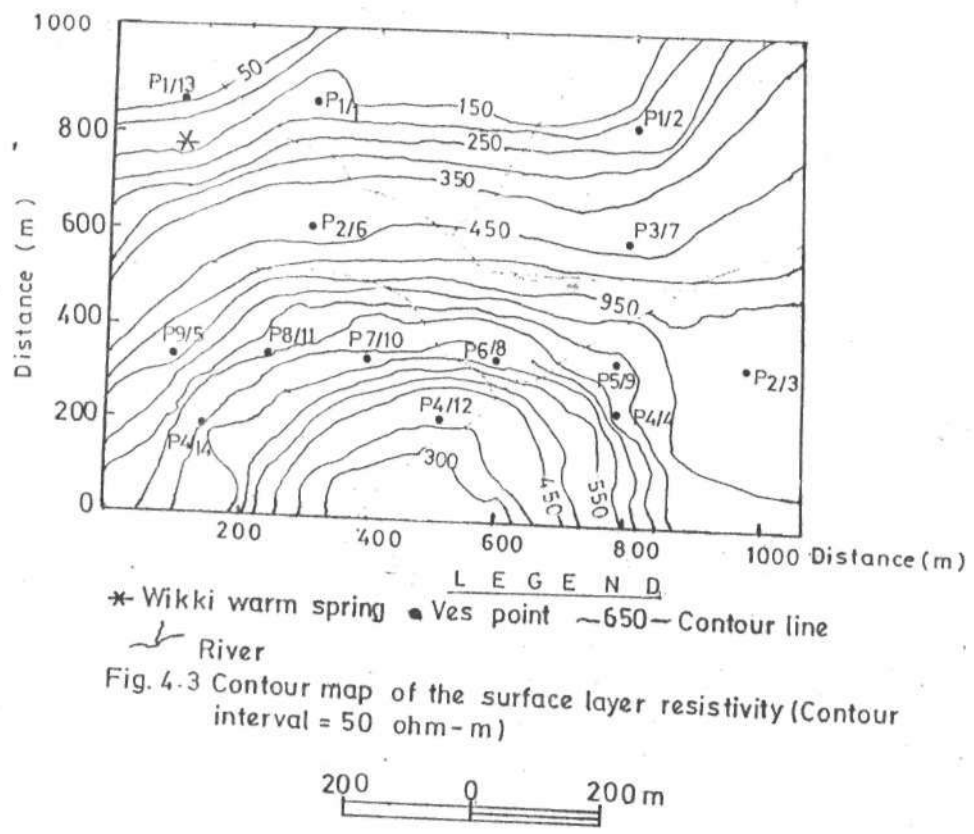


Fig. 4.3 Contour map of the surface layer resistivity (Contour interval = 50 ohm-m)

Table 4.1: Resistivity values for sedimentary rocks (Telford, *et al.*, 1975).

Rock type	Resistivity range (Ω-m)
Consolidated shales	$20 - 2 \times 10^3$
Conglomerates	$2 \times 10^3 - 10^4$
Sandstones	$1 - 6.4 \times 10^8$
Dolomite	$3.5 \times 10^2 - 5 \times 10^2$
Alluvium and sands	10 - 800

Table 4.2: Resistivity values used in deriving the geologic sections in this work (Telford, et *al.*, 1975).

Rock type	Resistivity range (Ω-m)
Consolidated shales	$20 - 2 \times 10^3$
Siltstones and mudstones	10 - 800
Sandstones	$1 - 6.4 \times 10^8$
Fresh Basement	> 1000

4.2.3 Geoelectric and Geologic Sections for VES Point P2/3, P5/9, P6/8, P7/10, P8/11 and P8/5

The composite geoelectric section derived for all the VES points is shown in Fig. 4.2a. The geoelectric section suggests that the subsurface along the VES points are made up of 3 layers. At these VES points, the resistivity of the upper layer ranges from 274-2,600 Ω-m with an average of 958 ohm-m. The thickness of this layer varies from 2.5m to 9.8m.

The second layer has a resistivity in the range 350 to 1620 ohm-m. This layer has the lowest resistivity values and hence, the most likely layer of the sandstone-shale junction which has several seepages. The thickness of the layer varies from 24.2m to 41.3m.

The third layer has relatively higher resistivity values throughout the VES points. The resistivity values of this layer ranges from 1500 to 2980 ohm-m. The geologic section derived from these VES points is shown in Fig. 4.2b based on resistivity values presented in Tables 4.1 and 4.2. The section suggests that the top most layer must probably consist of two different soil types. The high resistivity zone (801 - 2600 Ω-m) of the layer occurring around VES P8/11 and P2/3 is considered to be consolidated shales. On the other hand, the zone with relatively medium resistivity values (27[illegible] - 800 Ω-m) occurring around VES P9/5 and between VES P7/10 and P5/9 is considered to be a layer of very saturated sandstones and sands based on Table 4.1.

The Figure also suggests that the second layer consists of two rock types. The first type found around VES P8/11 and P7/10 with a resistivity range of between 350-480 ohm-m may suggest a layer of consolidated shales. The second type which lies around VES P6/8 and P2/3 may be considered to be a layer of the porous sandstone sequence with resistivity values (920 - 1620 Ω-m).

The third layer whose resistivity values range from 1500 - 2980 Ω-m is considered fresh basement.

4.3 Maps Produced from Interpreted Data

In order to clarify certain aspects of the study area, resistivity and isoresistivity maps were produced from the interpreted resistivity data of the whole area. Though possible interpretations have been given, each of the maps discussed below show the whole area at a glance. The different types of maps produced are briefly discussed below.

4.3.1 Resistivity Map of the Surface Layer

This map was produced by contouring the resistivity values obtained for this layer at all the VES points. The resulting map (Fig. 4.3) was drawn with a contour interval of 50 Ω-m. This map is meant to show the variation of resistivity of the topmost layer, which could be used to compare with the surface features (such as the streams, rivers and warm springs).

The Figure shows that the resistivity values of the topmost layer in the study area range from 160 Ω-m at around

VES P1/13 to 3306 ohm-m which could be the sandstones sequence at around VES P4/4. VES points P1/1, P1/2 and P1/13 have the lowest resistivity values on the map, which may suggests that the soil cover in this area is most probably filled with fluid.

4.3.2 Isoresistivity Map at AB/2 = 25m and at AB/2 = 35m

The maps (Fig. 4.4a,b) were prepared using resistivity values obtained for AB/2 = 25m and AB/2 = 35m for various VES points. These maps were prepared at these depths to see how the resistivity of the major component (sandstone sequence) of the aquifer in the area varies from place to place at these depths with the aim of delineating the most likely area(s) of water saturation.

The Appendix A shows the plotted apparent resistivity versus AB/2 curves in the region. The curves show that the lowest resistivity values are usually recorded between AB/2 = 25m and AB/2 = 35m. This is suggestive that the region is most likely saturated with water. Hence the decision to investigate this region with more detail through the production of maps shown in Figs. 4.4(a) and (b). The two Figures are approximately similar to each other. Each of the maps suggest the existence of two similar anomalies which are labelled X and Y in Figure 4.4a and X^1 and Y^1 in Fig. 4.4b. The resistivity values in these regions range from 120 ohm-m and 800 ohm-m in the two maps. These regions with low resistivity values could be favourable for water accumulation.

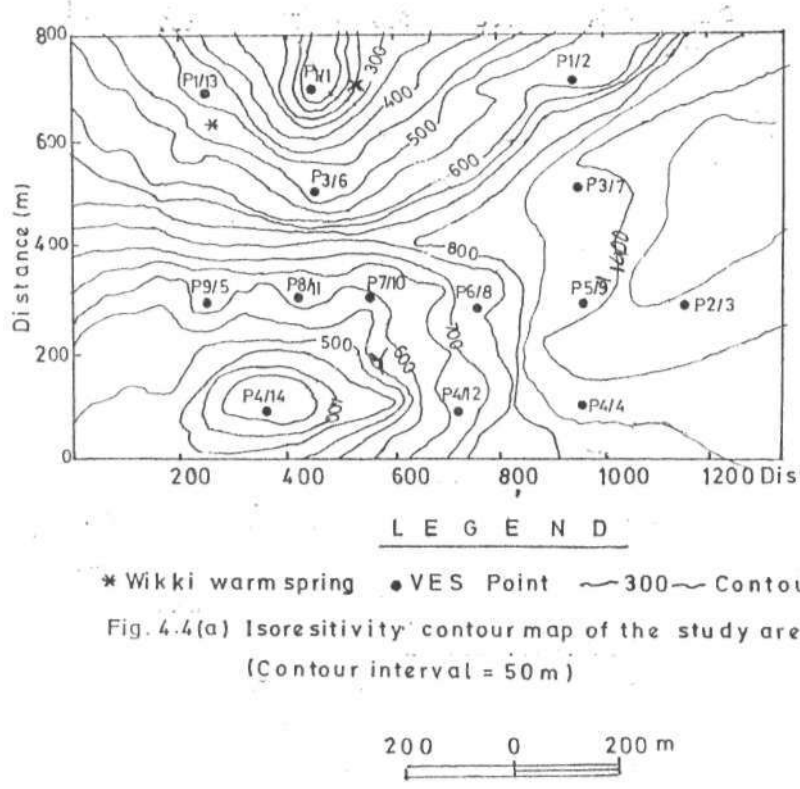


Fig. 4.4(a) Isoresistivity contour map of the study area at $\frac{AB}{2}$ = 25 m
(Contour interval = 50 m)

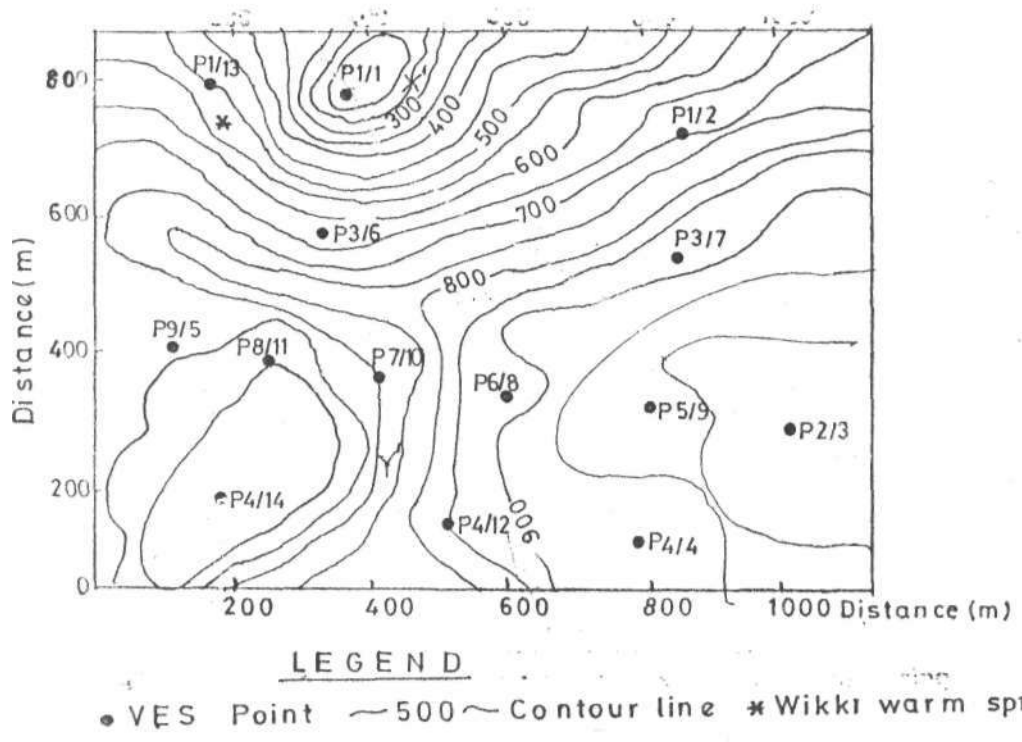
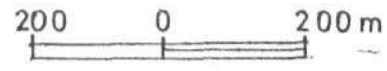


Fig. 4.4b Isoresisitivity contour map of the study area at $\frac{AB}{2}$ = 35m (contour interval = 50)



Low apparent resistivity values are always associated with warm or hot waters (Dounas *et al.*, 1972). The low apparent resistivity values obtained at VES points P1/1, P1/2, P1/13 are surface measurement. If these low values of resistivity are however obtained at greater depths, then it could probably indicate that the source heat of the Wikki warm spring may be 100m and even further away from the Wikki warm spring.

4.4 Results of Radioactivity Measurements

Heat due to the decay of radioelements can be great enough to account for the source of heat for hot springs (Birch, 1954). To investigate the contribution of the radioelements to the source heat in warm springs of the Yankari area, a gamma-ray survey of the Wikki warm spring area was undertaken. In addition, the contribution of the three radioelements (Thorium, Uranium and Potassium), to the overall radioactivity of the area was determined by gamma-ray spectrometry in which the gamma activity due to each of this nuclides was obtained.

The results of gamma-ray spectrometric survey of an area can be presented in any one or all of the following ways:

(a) a contour map showing areas of equal count rates or

(b) a contour map showing areas of equal radioelements concentrations (%k) for Potassium and in parts per million (ppm) for Uranium and Thorium, or

(c) a contour map showing areas of equal uranium to Thorium ratio (U:Th) or Uranium to Potassium ratio (U:k) or Thorium to Potassium (Th:k) ration.

Based on some analyses, areas of possible radioelement importance can be delineated from such contour maps.

The concentrations of all these radioelements for all the sample points along profile P1 are given in Table 4.3 while those for profiles P2 - P9 are given in Appendix B.

The total count map, Fig. 4.5 shows that the anomalous gamma-ray counts occur at the north-eastern and north-western parts of the project area along the head of the Wikki warm spring. For the anomaly at the north-eastern part of the area, the peak intensity (highest contour value) is 2100 c/s. For the anomaly at the north-western part of the area, the peak intensity is 2000 c/s. These areas as shown in the Figure occur across the head of the Wikki warm spring. Generally, the total count map (Fig. 4.5) shows high count rates throughout the study area. If the high gamma activity persist at greater depths then, the importance of radioactivity as contributory to the heat source at Wikki warm spring can be appreciated. It has been shown from other studies that gamma activity increases with depth. Therefore, at greater depths at Wikki warm spring area, the gamma activity may be higher than the values obtained at the surface. This may thus indicate the importance of radioactivity to the source heat of the Wikki warm spring.

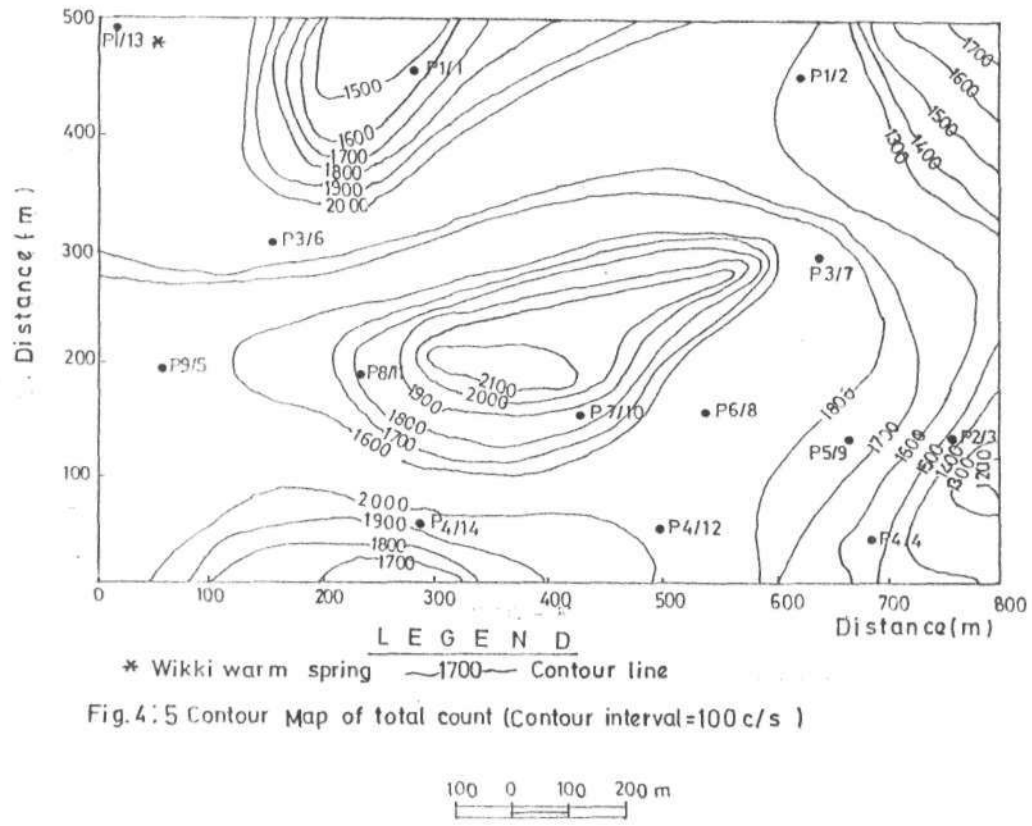


Fig. 4.5 Contour Map of total count (Contour interval=100 c/s)

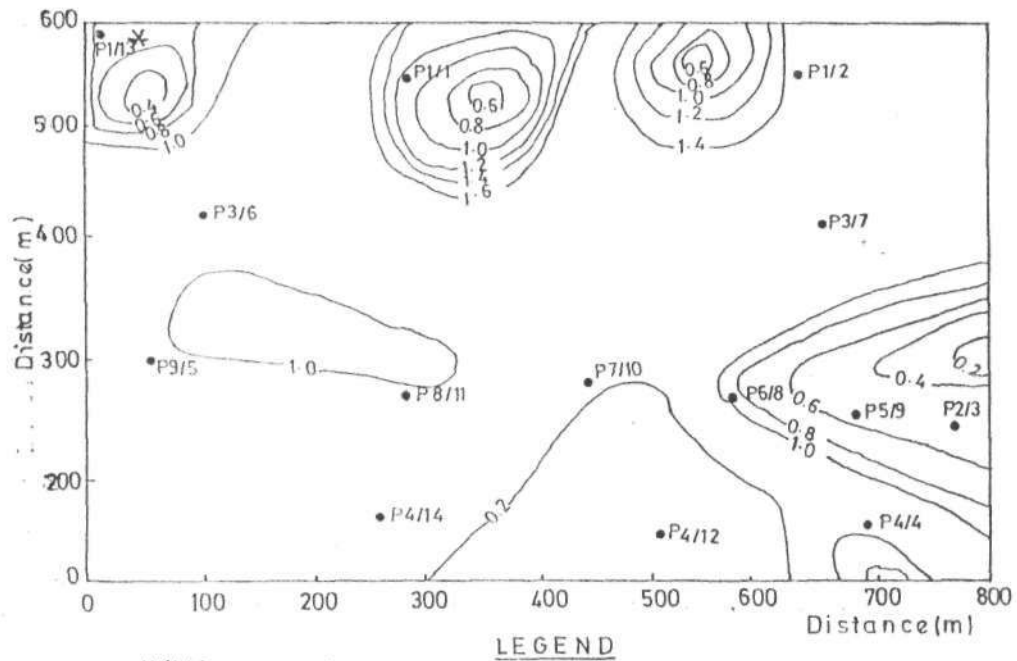
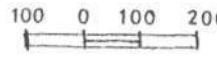


Fig 4.6 Contour Map Showing % Potassium Concentrations
(Contour Interval = 0·2 %)



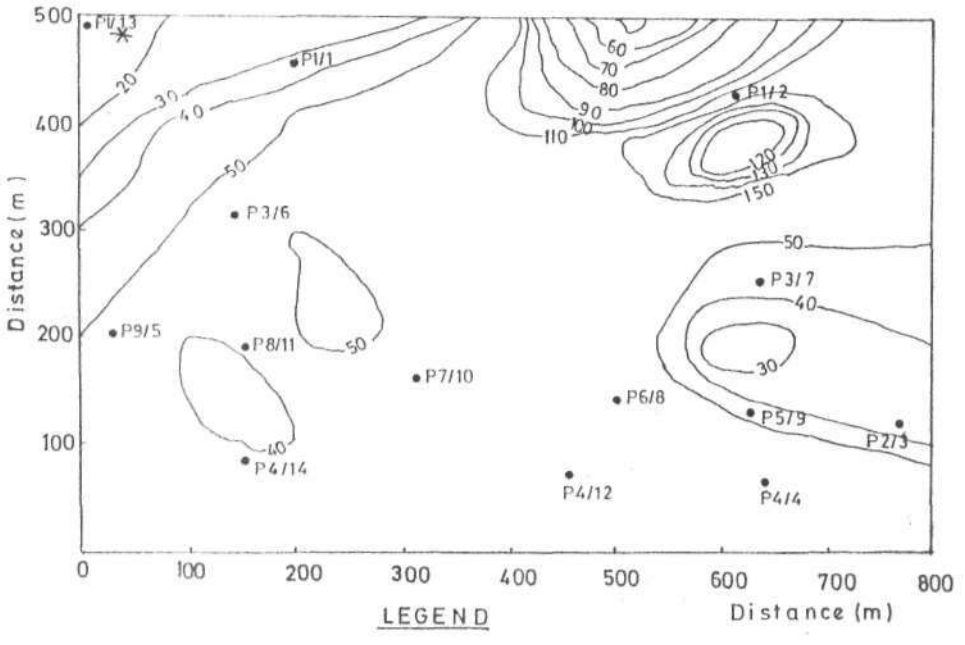


Fig. 4.7 Contour Map Showing e^{U} Concentrations (Contour Interval = 10ppm)

100 0 100 200 m

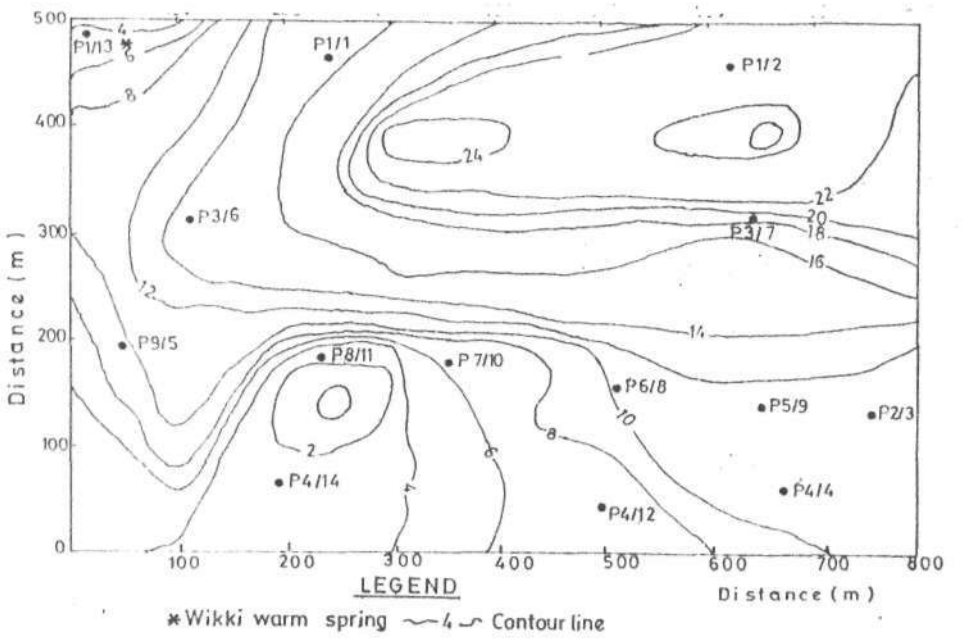


Fig. 4.8 Contour Map Showing e^{Th} Concentrations (Contour Interval = 2 ppm)

100 0 100 200 m

Fig. 4.6, 4.7 and 4.8 show the contour maps for Potassium, Uranium and Thorium concentrations respectively. The contour maps of the individual elements also reveal some anomalies. The anomalies in the %k map are coincident with the *e*U anomalies. These anomalies occur at the north-eastern and north-western parts of the study area. The peak or highest contour value of %k for the area is 1.6 while that of *e*U is 154 ppm. Thorium concentrations as shown in Fig. 4.8 also contribute to the total radioactivity of the area. From these Figures and the computed values of the area. From these Figures and the computed values of the individual element concentrations, the three radioelements were identified as the source of radioactivity in the area.

Table 4.3: The concentration of gamma-ray activity in the Wikki area (Profile 1).

Station	%k	*e*U (ppm)	*e*Thu (ppm)
1	1.0	29	4
2	1.0	29	4
3	0.8	29	15
4	0.6	30	16
5	1.2	50	18
6	1.2	50	18
7	1.2	95	22
8	1.4	95	22
9	1.3	56	22

The high gamma activity occur across the head of the Wikki warm spring. Further away from the Wikki warm spring, the activities increase. The reference background for each

of the three elements were calculated. It was observed that the gamma activity in the Wikki area is above normal. This high surface value of gamma activity in the Wikki area, if it persists at greater depths, then it may suggest that the heat from radioactivity contributes to the observed higher than normal water temperature. The average Potassium contribution in granites is about 4.0% (Clark, 1966). However, 1% value obtained in some stations in this work is enough to contribute to the observed warmth in the Wikki spring water if this 1.0% is also obtained at greater depths. It is, therefore, apparent from the results presented in Table 4.3, Appendix B and Fig. 4.5, 4.6, 4.7 and 4.8 that the source of heat of the Wikki warm spring may be due to high radioactivity of the area if the surface measurements persist at greater depths. That is, combining the heat produced by the three radioelements in the Wikki area, it is enormous enough to heat the water in the spring to a temperature of 31.1°C.

Chapter Five

DISCUSSION, SUGGESTIONS AND CONCLUSION

5.1 Discussion

Based on the interpretations presented in Chapter Four, a number of deductions can be made. Such deductions may include the probable source of heat, the pattern of apparent resistivity values as it relates to the probable area where the heating takes place.

Results of the electrical resistivity sounding survey in this study as presented in Figures 4.1 and Appendix A indicate rather low resistivity values in the area. Fig. 4.1 shows that the resistivity values of the topmost layer in the study area range from 160 ohm-m at around VES P1/13 to 3306 oh-m at around VES P4/4. VES points P1/1, P1/2 and P1/3 have the lowest resistivity values on the map, which probably suggests that the soil cover in this area is most probably filled with warm water. These low resistivity values were however recorded further away from the point where water is gushing out from the spring. This low values of resistivity could suggest that the source of water could be further away from the location of the Wikki warm spring.

The report of the divers of Warri, Delta State in 1986 who actually carried out an investigation to identify the source of water for the management of Yankari National Park, discovered that there was no temperature change in water in

the spring even some 9m away from the point where the water gets into the spring. This fact notwithstanding, moreso as the Wikki warm spring flows beneath deep layers of earth crust as far away as south east plateau region of Nigeria (Ike *et al.*, 1988), the source water may be very distant away from the site of the spring.

Results from the radiometric survey as reported in Chapter Four show high gamma activity. Around the head of the spring for example, high gamma activity were recorded revealing some radiation anomalities even further away from the site of the spring. Also further away from the Wikki warm spring the surface activity increases. All these go to suggest that the source heat in the spring is at a distance from the location of the spring. Although as shown the source of water is much further down and away from the location of the spring, and also surface radioactivity may not be more than 1m below the point of measurements, the generally high values of gamma activity may suggest the importance of radioelements to the source of heat in the Wikki warm spring area.

5.2 Conclusion

In this work, two methods of geophysical surveys (resistivity and radiometric surveys) were carried out to investigate the possible origin of the source of heat which heats the water in the Wikki warm spring. The survey was also concerned with the point where this heating takes place; that

is, whether the water is heated in the immediate vicinity of the spring or at some distant point.

The electrical resistivity sounding results showed rather low resistivity values (105 ohm-m to 305 ohm-m) in the Wikki area. Low resistivity values also occur further away from the point where water is gushing out from the spring suggesting that the source water is further away from the location of the Wikki warm spring, VES point P1/1 is located 300m away from the head of the Wikki warm spring. It has low resistivity values throughout its layers and the depth to the basement was obtained to be 16.2m.

Results from the radiometric survey carried out in this work show high gamma activity. The higher than the average radioactivity in the area indicates the importance of radiogenic heat in the Wikki warm spring area. Results also show high radioelements concentration, potassium, uranium and thorium in the area. The radioelements may have higher concentration at depths as discussed in the preceding section which suggests the high contribution of radiogenic heat in the region. Results from the study showed that both source of water charging the spring and the heating of the water as obtained, occurred at some distance away from the spring.

5.3 Suggestions for Further Work in the Area

As in all methods of geophysics, the electrical and radiometric methods of survey used here cannot give complete information about the source of heat in the Wikki spring.

Hence, the information obtained in this work should be supplemented and complemented with those that can be obtained using other methods of geophysical prospecting. Notable among these methods is the seismic method. A seismic refraction survey is capable of unambiguously delineating the buried structure within the spring.

Secondly, the study of the ratio of the isotopes of hydrogen and oxygen in water should be carried out to determine the origin of water in the spring. Such a study will reveal whether the water is coming from the interior of the earth or derived from underground water. That is, whether it is of meteoric origin or otherwise.

On a final note, a detailed geochemical survey can also be carried out to determine the type, mode of occurrence of the water and for determination of concentrations and ionic ratios of important dissolved and gaseous constituents of the water. These may include the analysis of the waters of the springs and streams and the sediments in the area.

REFERENCES

Anovski, T.J., Karcurkov, D., Kirkov, P. and Tolev, M. (1965). Determination of the origin of water in springs from the simultaneous application of natural and artificial isotopes; some aspects of the origin of water in the Rashe spring. Geophysics Vol. 26 pp. 125-141.

Batchelor, A.S. (1982). The Stimulation of a hot dry rock geothermal reservoir in the cornubian granite, England: in Proc. Eighth workshop Geoth. Reservoir Eng., Stanford Univ., Stanford, California, SGP-TR-60.

Banwell, C.J.(1961). Geothermal drill-holes: Physical investigations. Proc. U.N. Conf. on new sources of energy, Rome, 1961, Vol.2, Pp 60 -72.

Birch,F (1954). Heat from radioactivity. In: Faul H. (Ed.) Nuclear geology, John Wiley and Sons, New York.

Bullard, E. (1968). Reversals of the earth's magnetic field. Phil Trans Roy. Soc. A, 263,481.

Bullard, E. (1969). The origins of the oceans. Soc. Amer. 221, 66. (Also appears in the scientific American publication "The oceans"). Hand book of physical constants. Men. Geol. Soc. Amer., No.97, pp. 459 - 482.

Clark, S.P. (1966). Handbook of physical contents. Mem. Geol. Soc. Amer., No. 97, p.459-482.

Costain, J.K., Glover, L. and Sinha, A.K. (1980). Low temperature geothermal resources in the Eastern United States, EOS, 61, Pp 1 - 13.

Darnley, A.G. (1972). Airbone gamma-ray survey techniques. In: Bowie *et al.* (Editors), Uranium Prospecting Handbook. Institute of Mining and Metallurgy, London, pp. 174-211.

Doig, R. (1968). The Natural gamma-ray flux: in-situ analysis. Economic Geology. Vol. 33, pp. 311-328.

Dounas, A., Stahl, W., and Aust, H. (1972). Origin of Artesian and thermal waters determined by oxygen, hydrogen and carbon isotope analysis of water samples from Sperkhios Valley, Greece. Geophysical prospecting, Vol. 36 pp. 213-236.

Ellis, A.J. (1975). The solubility of calcite in carbon dioxide solution. American Scientist, Vol.63, pp. 515.

Fargher, M.N. (1961). Yankari Game Reserve Wikki Warm Spring. (Unpublished report presented to the management of the Yankari National Park).

Frischknetcht, F.C. and Keller, G.V. (1966). Electrical methods in geophysical prospecting, Permamon Press, New York Pp. 517.

Geometrics, (1984). Model DISA-300 Gamma-ray Spectrometer Operating Mannual.

Holmes, A. (1964). Principles of physical geology, London, Nelson, 1088P.

Ike, E.C., Schoeneich, K., Woakes, M., Ezealor, U.A.,(1985). An assesment of the Yankari National Water Company operational on the Yankari Game Reserve, Bauchi State. Unpublished report prepared by the Geology Dept., A.B.U. for Bauchi State ministry of commerce, industry and co-operative.

Ike, E.C., Schoeneich, K, and Woakes, M. (1988). Water resource management for the Yankari Game Reserve, Bauchi State, Nigeria. Paper presented at the Nigerian Association of Hydrogeologist International water resource conference, at Geology Dept., University of Benin, Nigeria, from 15th to 19th Nov. 1988.

Jeffreys, H.(1970). The Earth (5th ed.). Cambridge University Press, 525p.

Keller, G.V.(1970). Induction methods in prospecting for hot water. U.N. symp. on geothermal energy. Pisa 1970.

Lee, W.H.K. (1965). Terrestrial heat flow. Washington, American Geophysical Union.

Lord Kelvin (1872). Changes in the convection pattern in the earth's mantle continental drift: Evidence for a cold origin of the earth. Phil.Trans.Roy.soc. London A 258,228.

McKenzie, D.P. (1968). The geophysical importance of high temperature creep. In: R.A. Phinney (Ed.). The history of the earth's crust, Priceton University Press, pp. 28 - 44.

Moscowitz, B. and Norton, D. (1977). A preliminary analysis of intrinsic fluid and rock resistivity in active hydrothermal system. J. Geophysics Res.82, Pp 5787 - 5795.

Roy, A. (1972). Depth of investigation in Wenner, three-electrode, and dipole-dipole resistivity methods: Geophysical methods: Geophysical prospecting, Volume 20, p. 329.

Roy, R.F., Blackwell, D.D. and Birch,F. (1968). Heat generation of the plutonic rocks and continental heat flow provinces on Earth Planet. Sci. Lett. 5,1.

Scintrex, (1973). Geophysical and Geochemical Instrumentation and Services. Model GIS-3 Gamma-ray Spectrometer User's Manual.

Smith,M.C. and Ponder,G.M.(1982). Hot dry rock geothermal energy development program. Annual report fiscal year 1981 Los Alamos Natonal Lab. Nm,(LA -9287 - HDR.

Telford, W.M., Geldart, L.P., Sheriff, R.E., and Keys, D.A. (1976). Applied Geophysics; Cambridge University Press, pp. 665-661.

Van Nostrand, R.G. and Cook, K.L. (1966). Intepretation of resistivity data. Prof. pap U.S. geol. surv.,449 Washington, U.S. Government Printing Office. (Library of Congress Catalog-Card No.G.S 65 - 322.

Wallace, R.H.Jr., Kraemar, T.F., Taylor, R.E. and Weesselman, J.B. (1979). Assesment of geopressured - geothermal resources in Northern Gulf of Mexico Basin: in Muffler, L.J.P., (Ed.), Assessment of Geoth. Res. of the U.S. Geol. Surv. Circular 790.

White, D.E., and Williams, D.L.(1975) Eds. Assessment of geothermal resources of the United States.

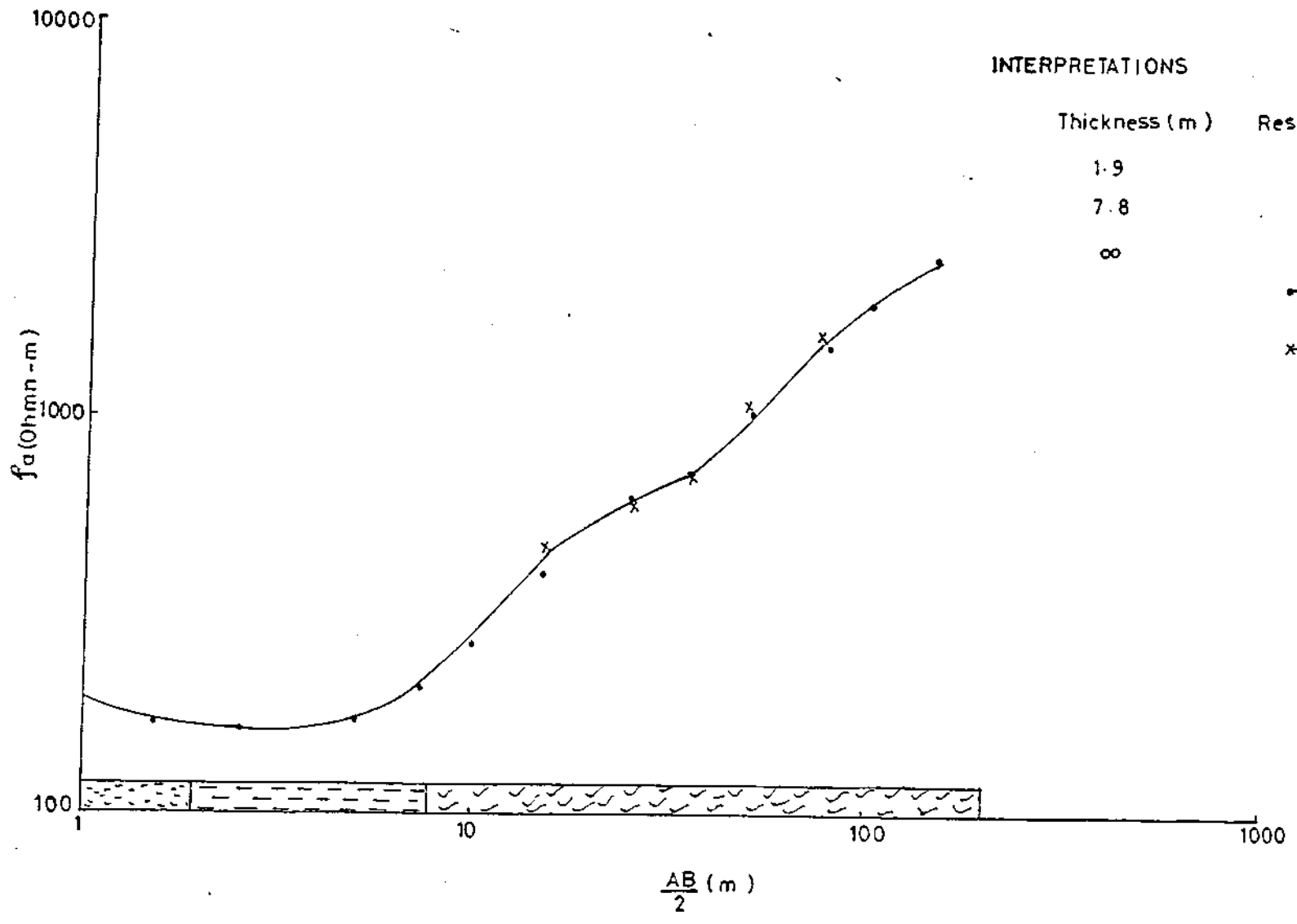
Whitely, R.(1973). Electrode arrays in resistivity and induced polarization prospecting, a review; Bulletin of the Australian society of exploration Geo-physicists, Vol.4, pp 1-29.

Williams, L.P. and Schersbatskoy (1951). Use of gamma ray detectors in prospecting. "Economic Geology" Vol.46, No.4.

Worthington, P.F. (1977). Geophysical Investigation of Groundwater Resources in the Kalahari Basin. Geophysics Vol. 42, pp. 838-849.

APPENDICES A

RESISTIVITY CURVES FOR THE VARIOUS VES POINTS IN THIS WORK.



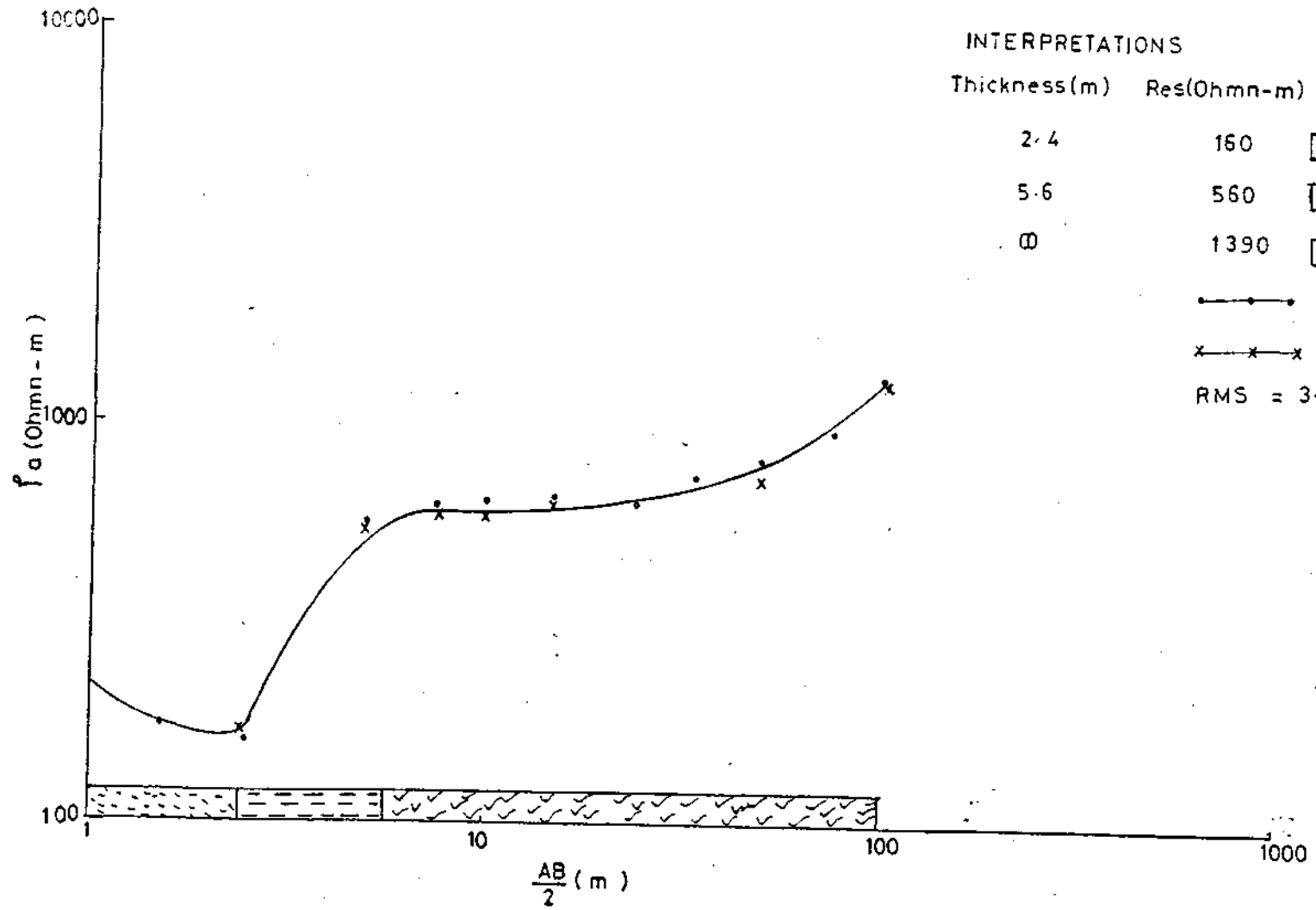
INTERPRETATIONS

Thickness (m)	Res (Ohmn-m)	Rock type
1·9	170	Clay Silt and mudstones
7·8	205	Sandstones
∞	2400	Fresh basement

Observed curve

Computed curve

RMS = 1.7



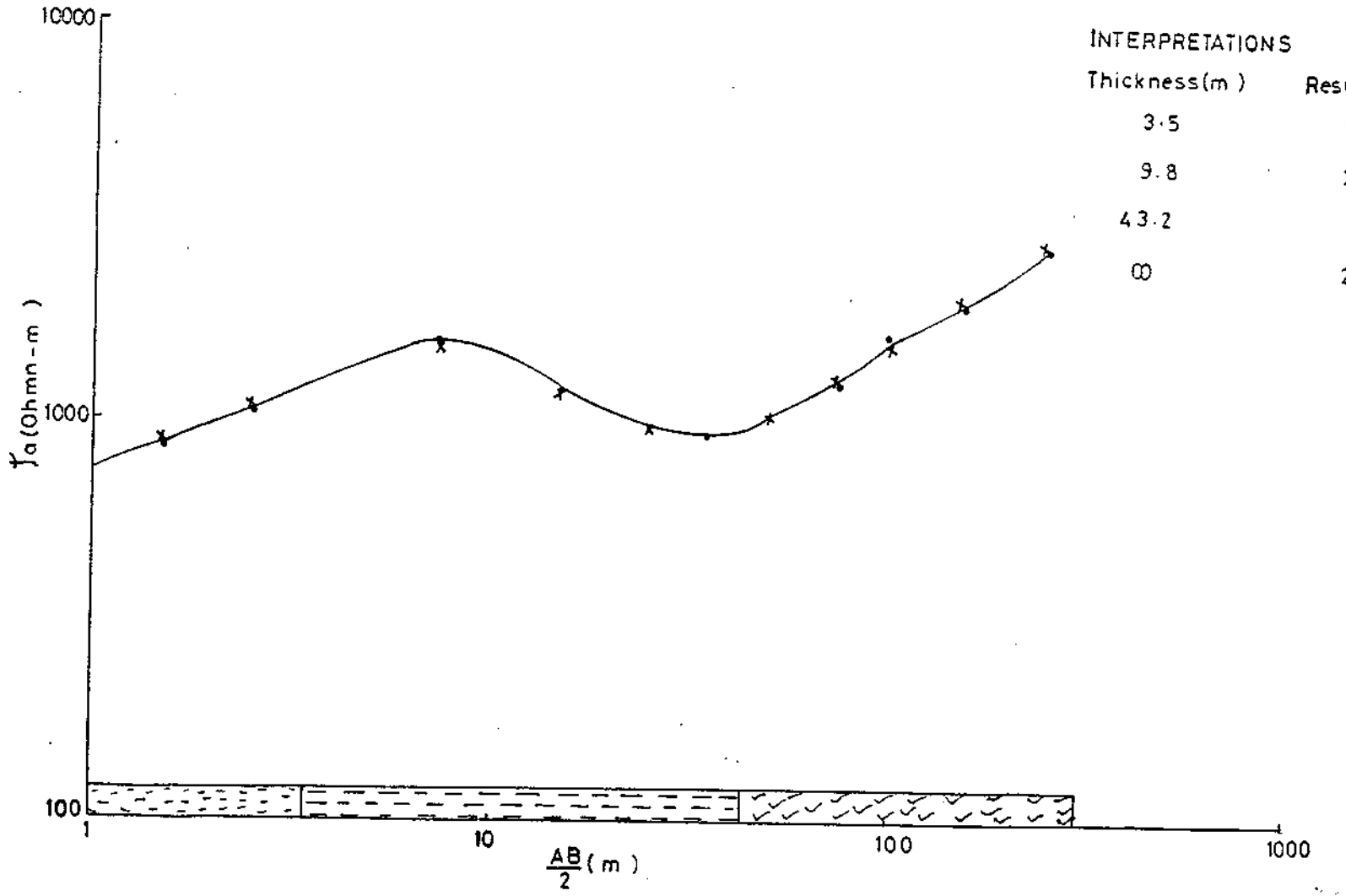
INTERPRETATIONS

Thickness(m)	Res(Ohmn-m)	Rock type
2·4	160	Claystones Siltstones Mudstones
5·6	560	Sandstones
∞	1390	Fresh basement

Observed curve

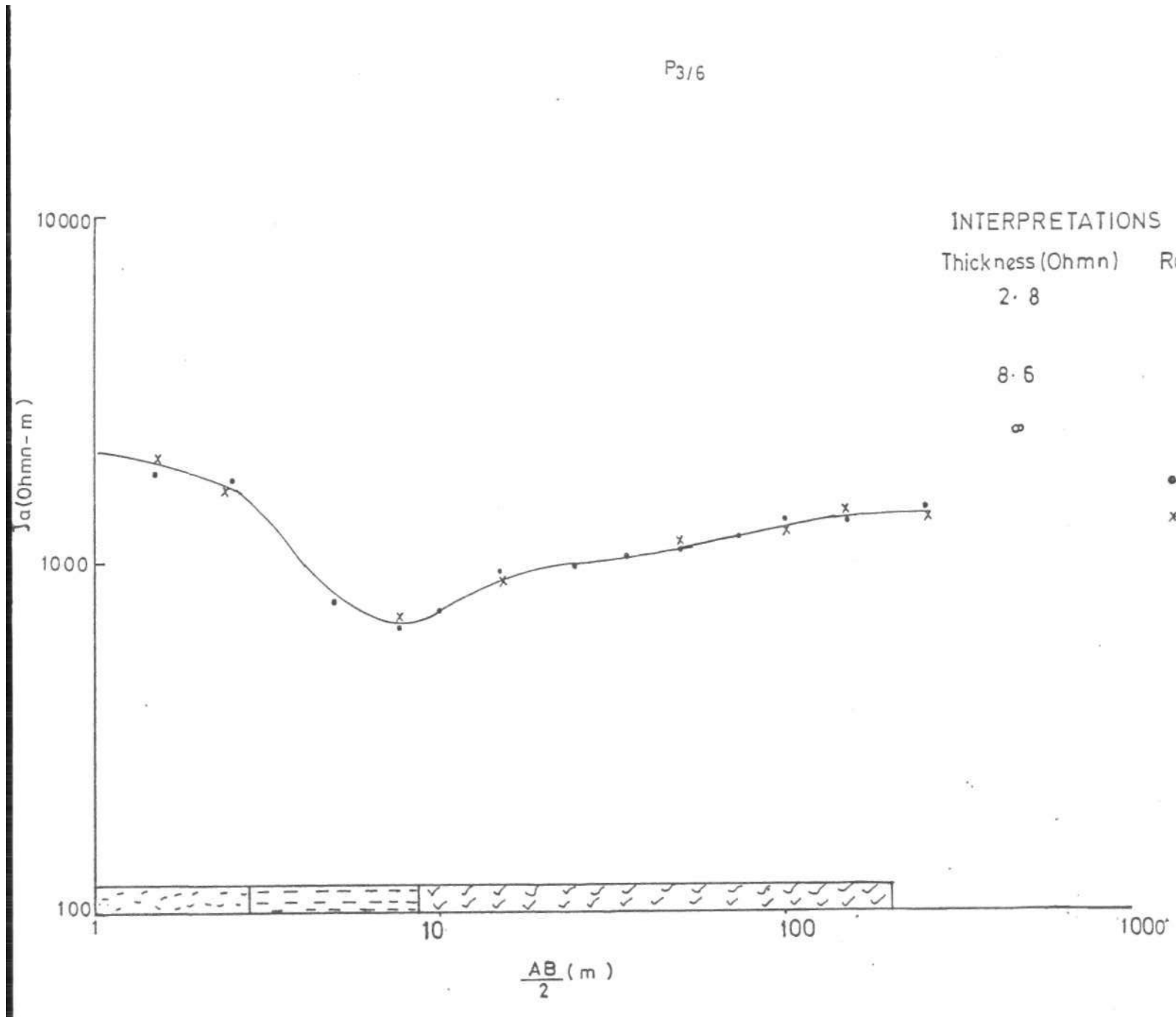
Computed curve

RMS = 3·1



INTERPRETATIONS

Thickness(m)	Res(Ohmn-m)	Rock type
3·5	1200	Claystones, Siltstones and Mudstones
9.8	2600	
43.2	960	Sandstones
∞	2980	Fresh basement



INTERPRETATIONS

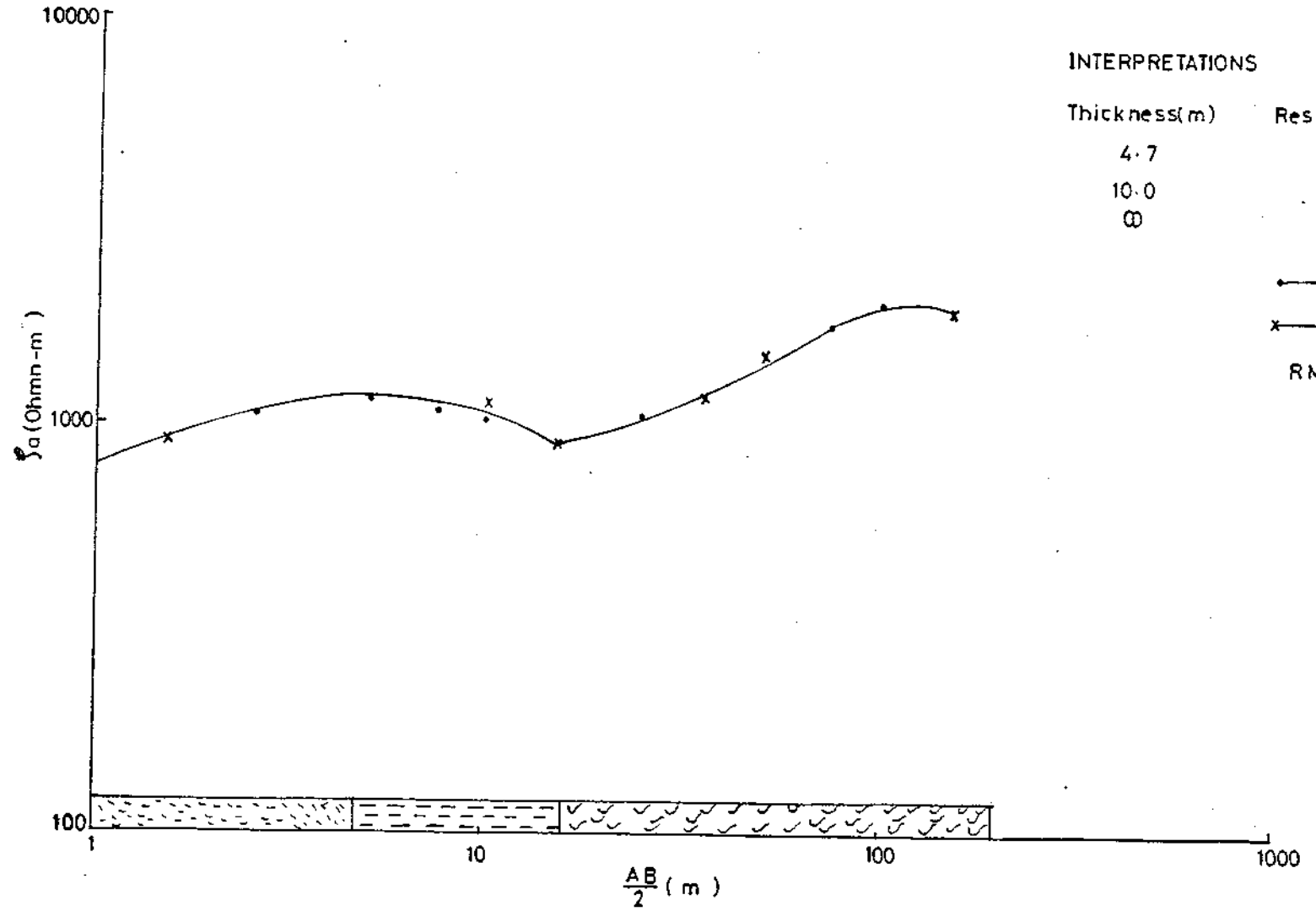
Thickness (Ohmn)	Res (Ohmn-m)	Rock type
2·8	1500	Claystones, Siltstones and Mudstones
8·6	680	Sandstones
∞	1460	Fresh basement

Observed curve

Computed curve

RMS = 2·3

$P_{3/7}$



INTERPRETATIONS

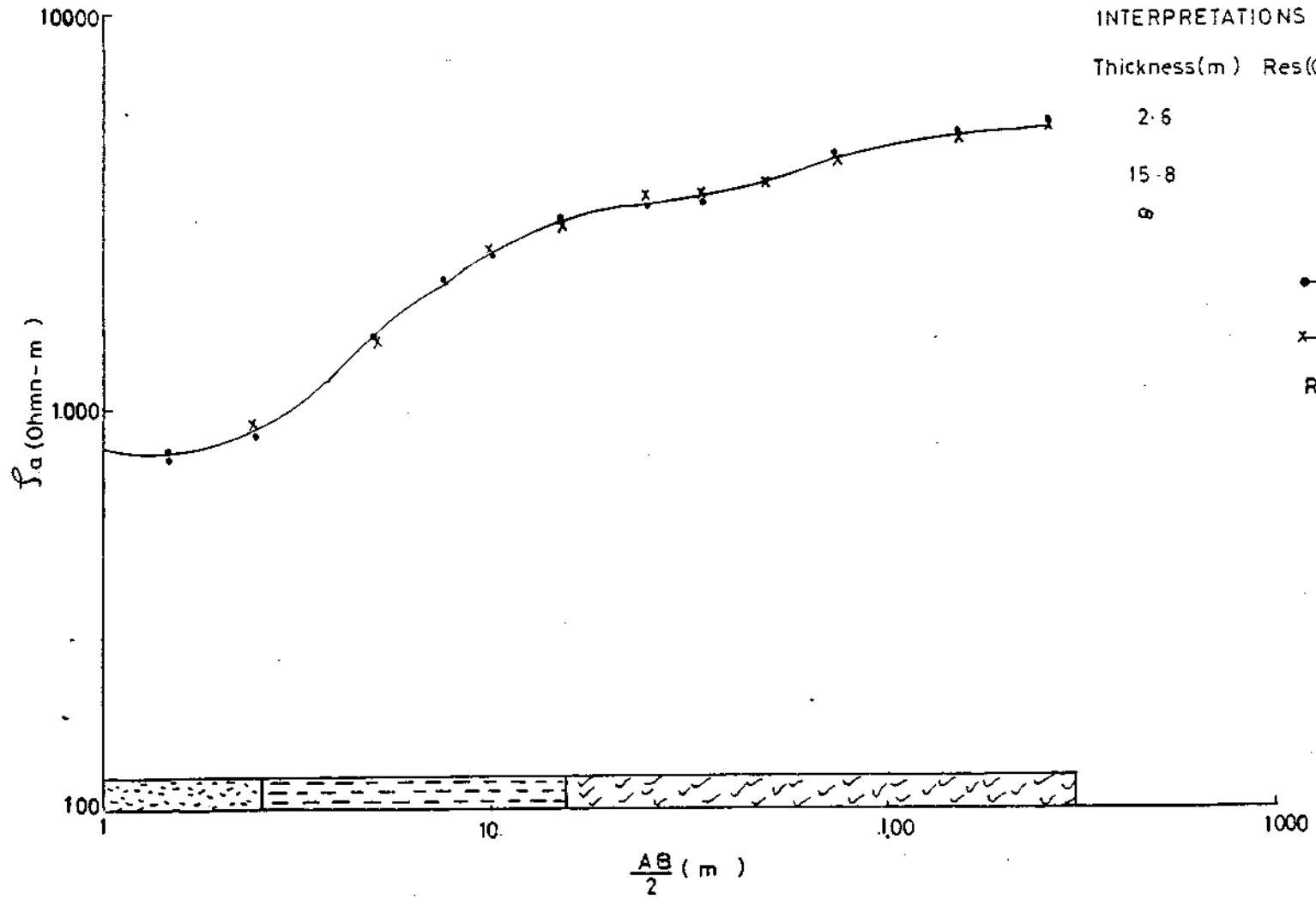
Thickness(m)	Res(Ohmn-m)	Rock type
4·7	1150	Clay, Silt, Mudstones
10·0	440	Sandstones
∞	1900	Fresh basement

Observed curve

Computed curve

RMS = 1·4

P414



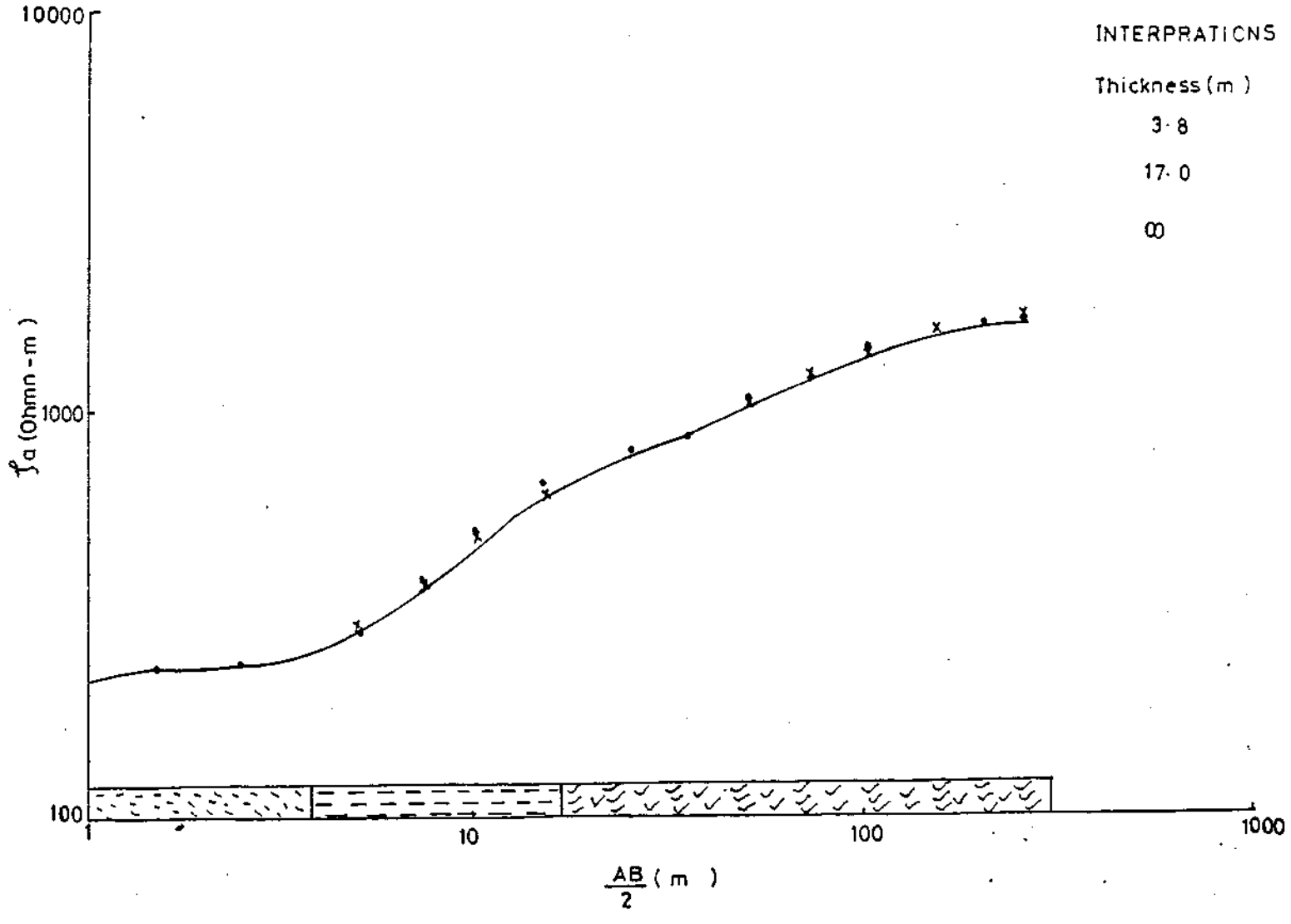
INTERPRETATIONS

Thickness(m)	Res(Ohmn-m)	Rock type
2·6	804	Claystones, Siltstones and Mudstones
15·8	3100	Sandstones
∞	4900	Fresh basement

Observed curve

Computed curve

RMS = 1.9



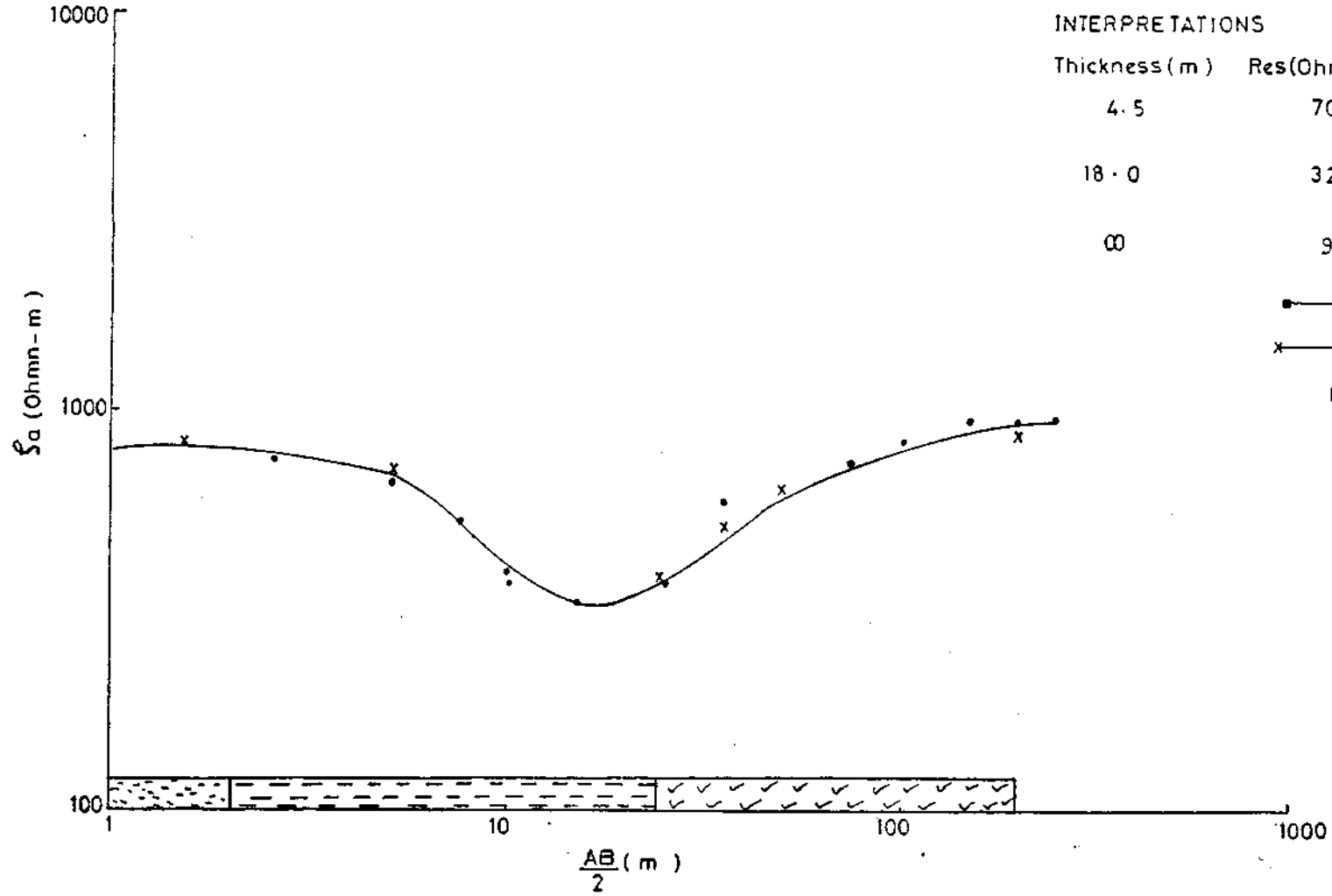
INTERPRATIONS

Thickness (m)	Res(Ohmn-m)	Rock type
3·8	260	Clay, Silt and mudstones
17·0	680	Sand stones
∞	1700	Fresh basemer

Observed curve

Computed curve

RMS = 2·7



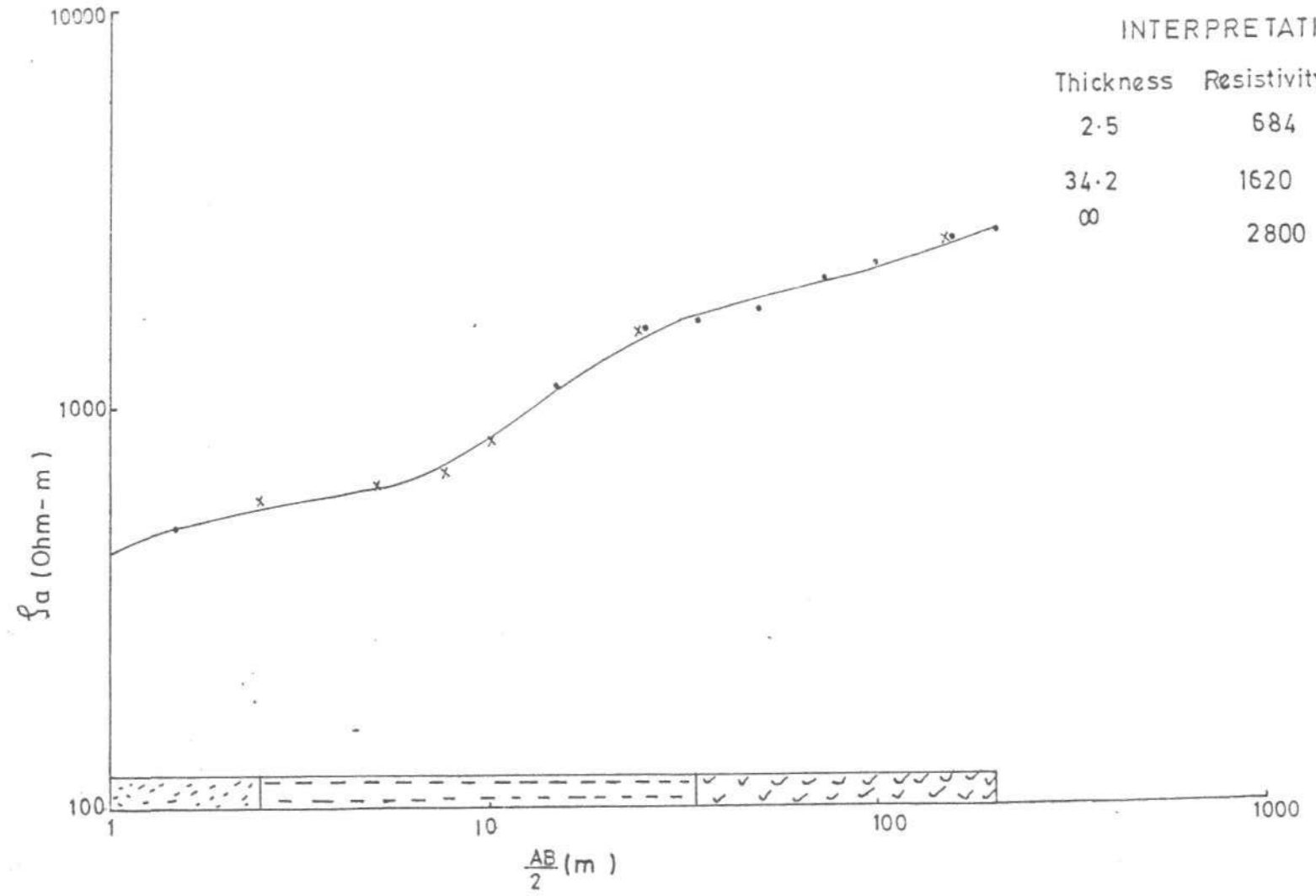
INTERPRETATIONS

Thickness (m)	Res(Ohmn-m)	Rock type
4·5	700	Claystones, Siltstones and Mudstones
18·0	320	Sandstones
∞	980	Fresh basement

Observed curve

Computed curve

RMS = 2·9



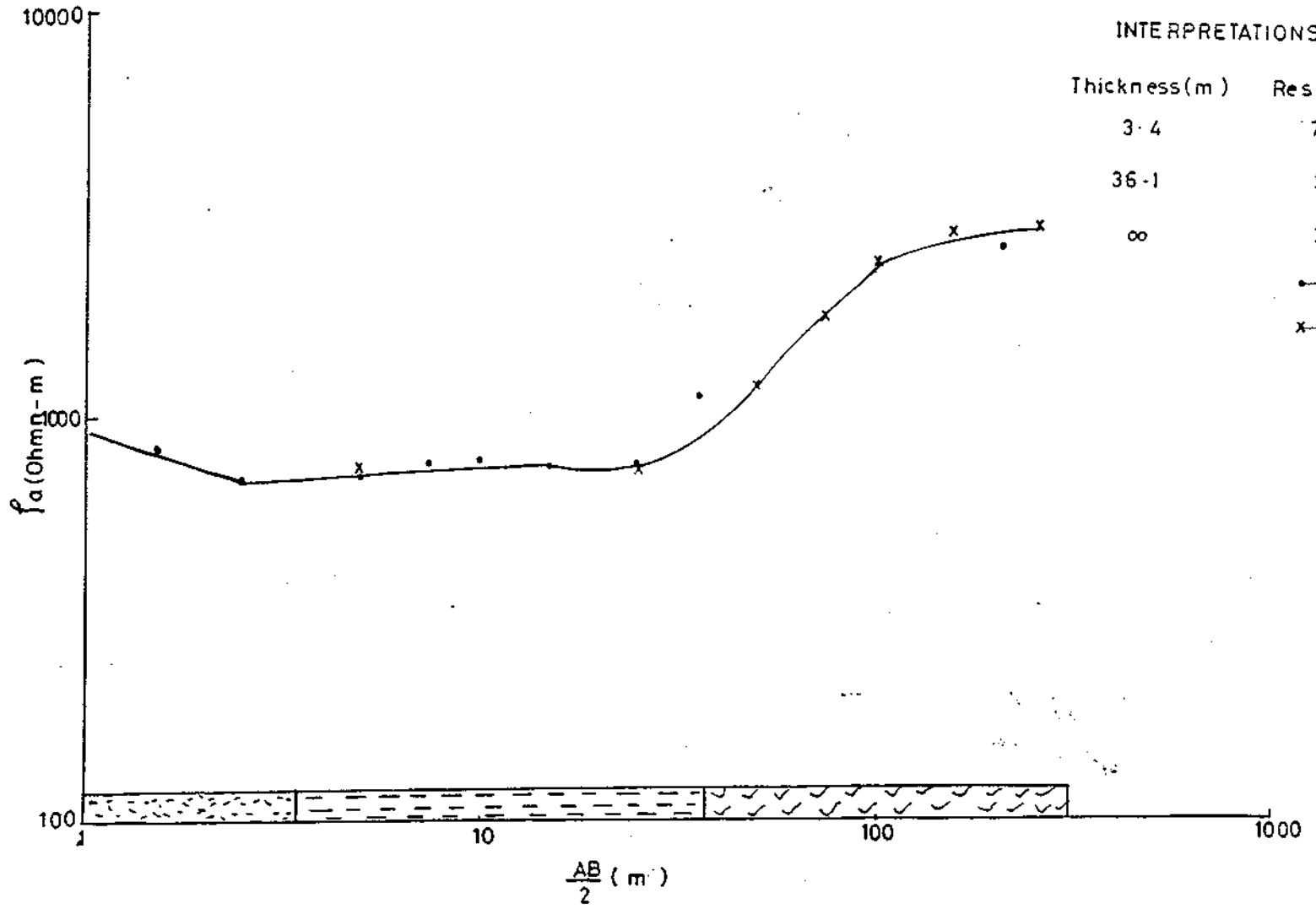
INTERPRETATIVE

Thickness	Resistivity (m)	Rock type
2·5	684	Claystones, Siltstones Mud.
34·2	1620	Sandstones
∞	2800	Fresh basement

Observed

Computed

RMS = 2·3



INTERPRETATIONS

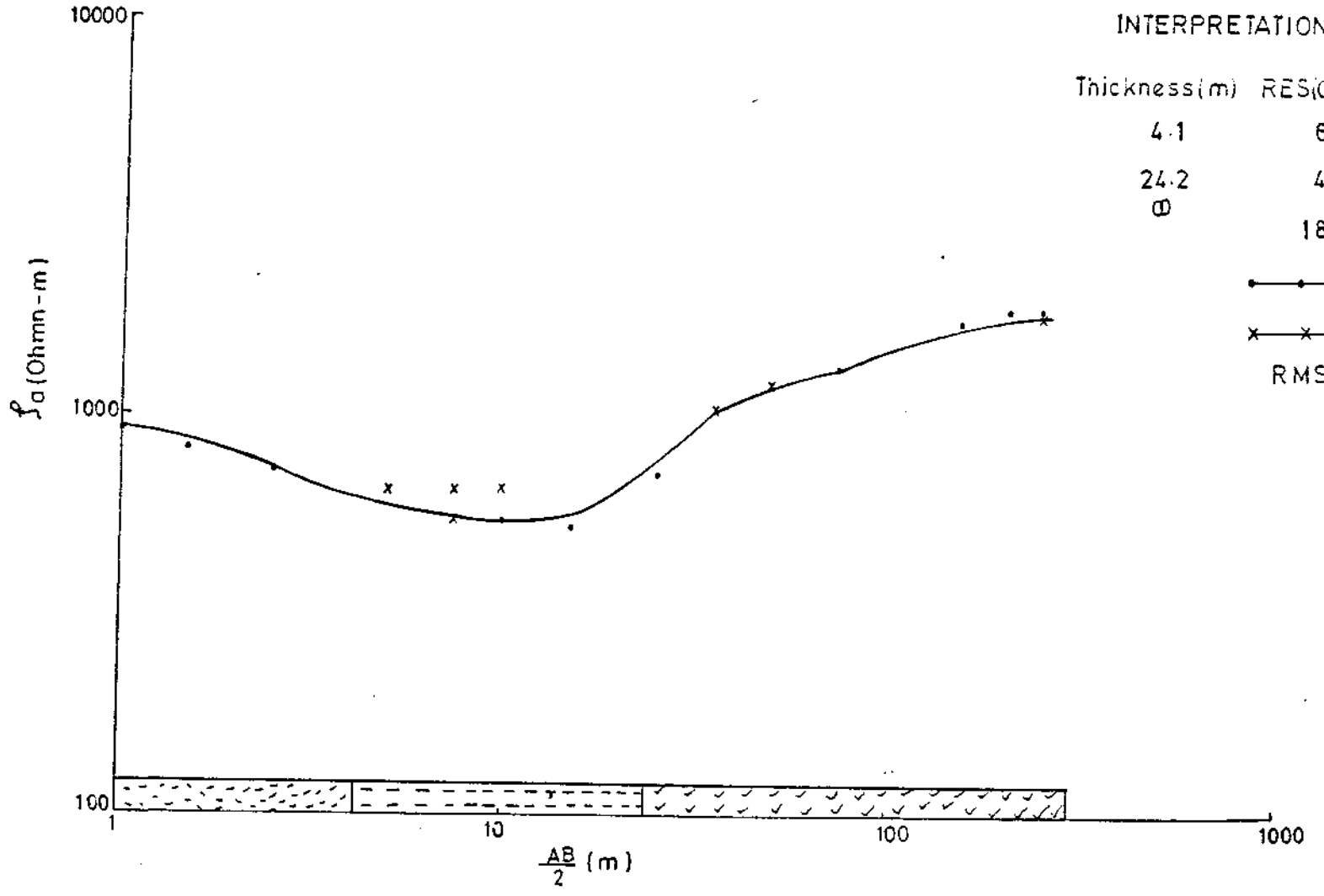
Thickness (m)	Res (Ohmn-m)	Rock type
3·4	720	Clay, Silt and mudstones
36·1	930	Sand stones
∞	2900	Fresh baseme

Observed curve

Computed curve

RMS = 2·4

P 7/10



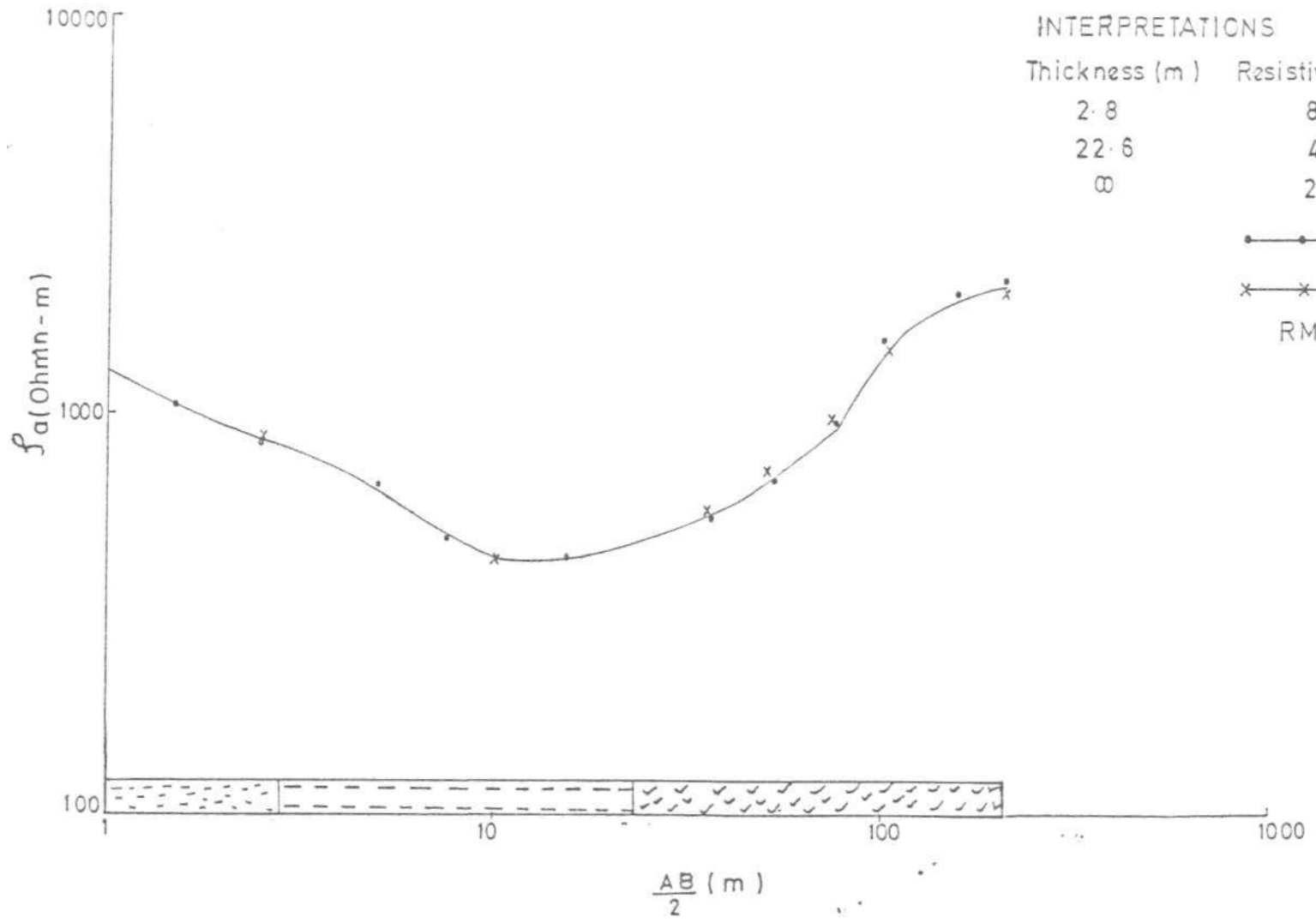
INTERPRETATIONS

Thickness(m)	RES(Ohmn-m)	Rock type
4·1	620	Claystones, Silt and Mudstones
24·2	480	Sandstones
∞	1880	Fresh basement

Observed curve

Computed curve

RMS = 2·1



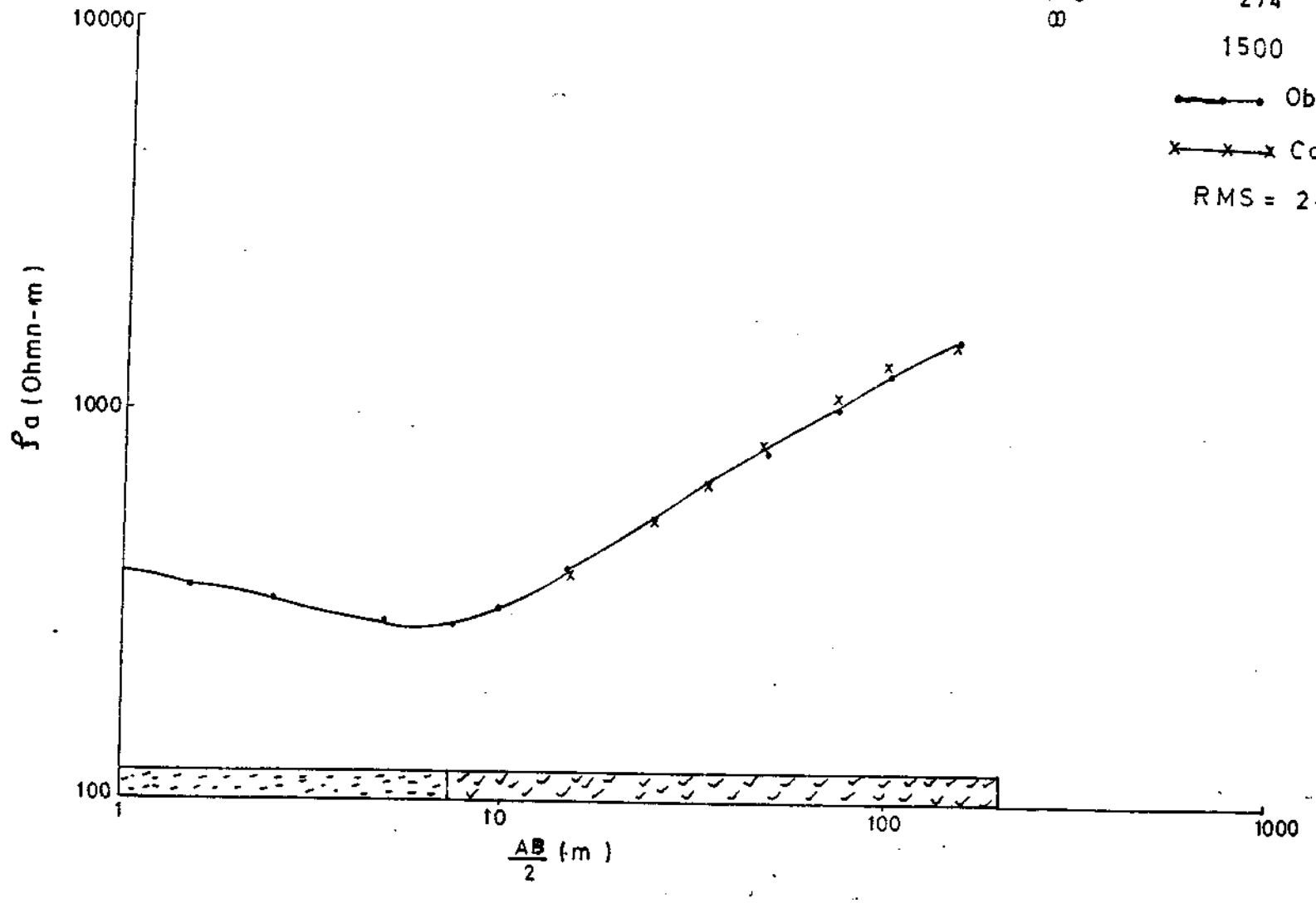
INTERPRETATIONS

Thickness (m)	Resistivity (Ohmn-m)	Rock type
2·8	820	Claystones, Siltstones and Mudstones
22·6	450	Sandstones
∞	2100	Fresh basement

Observed curve

Computed curve

RMS = 1·2



INTERPRETATIONS

Thickness(m)	Res(Ohmn-m)	Rock type
7·5	274	Claystones, Siltstones & Mudstones
∞	1500	Frash basement

Observed curve

Computed curve

RMS = 2·4

APPENDICES B

The concentrations of gamma-ray activity in the Wikki area (Profile P2)

Station	%k	eU (ppm)	eTh (ppm)
1	1.3	58	22
2	1.2	54	20
3	1.0	50	20
4	0.8	44	17
5	0.6	40	14
6	0.2	22	10

The concentrations of gamma-ray activity in the Wikki area (Profile P3)

Station	%k	eU (ppm)	eTh (ppm)
1	0.2	22	10
2	0.4	24	10
3	0.1	24	8
4	1.4	28	10
5	-	20	6
6	-	17	4
7	0.1	16	3
8	0.1	15	4
9	0.2	14	2

The concentrations of gamma-ray activity in the Wikki area (Profile P4)

Station	%k	eU (ppm)	eTh (ppm)
1	1.0	20	8
2	1.0	50	12
3	-	50	16
4	1.6	112	24
5	1.6	114	24
6	1.4	154	39
7	1.0	128	29
8	1.0	126	27
9	1.2	54	20

The concentrations of gamma-ray activity in the Wikki area (Profile P5)

Station	%k	eU (ppm)	eTh (ppm)
1	0.8	29	15
2	0.6	25	13
3	-	50	16
4	-	30	2
5	0.4	28	2
6	0.2	22	2

The concentrations of gamma-ray activity in the Wikki area (Profile P6)

Station	%k	eU (ppm)	eTh (ppm)
1	0.6	30	16
2	0.4	28	12
3	0.3	25	14
4	-	30	16
5	0.2	32	18
6	0.2	14	2

The concentrations of gamma-ray activity in the Wikki area (Profile P7)

Station	%k	eU (ppm)	eTh (ppm)
1	1.0	29	4
2	1.0	50	12
3	1.4	56	18
4	1.0	54	19
5	0.8	45	10
6	0.1	16	3

The concentrations of gamma-ray activity in the Wikki area (Profile P8)

Station	%k	eU (ppm)	eTh (ppm)
1	0.4	38	7
2	0.6	40	10
3	1.0	54	19
4	1.0	54	18
5	0.4	28	2
6	0.2	24	3
7	0.4	27	8
8	0.2	23	6
9	0.2	22	10

The concentrations of gamma-ray activity in the Wikki area (Profile P9)

Station	%k	eU (ppm)	eTh (ppm)
1	0.2	14	2
2	0.2	15	1
3	0.4	38	7
4	0.6	32	10
5	1.0	20	8
6	1.0	16	4